Anticorrosion and physico-mechanical properties of organic coatings with perovskites treated PANI and PPY phosphate layers

[a]Hájková T., [a]Kalendová A., [a]Kohl M., [b]Stejskal J.

[a] *Faculty of Chemical Technology, Institute of Chemistry and Technology of Macromolecular Materials, University of Pardubice, Studentská 573, 532 10 Pardubice, Czech Republic*

[b] *Institute of Macromolecular Chemistry, Academy of Sciences of the Czech Republic, 162 06 Prague 6, Czech Republic*

Corresponding author: Ing. Tereza Hájková, hajkova.ttereza@seznam.cz; Correspondence Address: University of Pardubice, Studentská 95, 532 10 Pardubice, Czech Republic

Received []

Abstract

This work describes the properties of perovskites pigments and subjected to surface treatment with conductive polymers for use in protective coatings. The perovskite type pigments (XYO_3; X = Zn, Ca Sr, Y = Ti, Mn) were synthesized by high-temperature solid-phase reaction, and their surface was modified with a conductive polymer, specifically polyaniline phosphate (PANI) or polypyrrole phosphate (PPY), by chemical oxidative polymerisation. Conductive polymers are currently attracting considerable interest in a number of sectors, among them the paint industry owing to their non-toxicity and high stability.

Paints consisting of a solvent-based epoxy-ester resin as the binder and the above-mentioned molybdate/PANI/PPY pigments were formulated and subjected to mechanical tests in order to assess the effect of the composite pigment particles on the paints' mechanical resistance. Anticorrosion efficiency of the paints was also examined in dependence on the type of particle surface treatment with the conductive polymer, chemical composition of the pigment, and pigment volume concentration (PVC) in simulated corrosive atmospheres. The effect of the surface-treated inorganic composite pigments on the corrosion rate was investigated by using electrochemical tests and accelerated corrosion tests.

Keywords: anticorrosion pigment, organic coating, conductive polymer, epoxy-ester resin, perovskites

Introduction

The most widespread method to protect the surfaces of metallic materials consists in coating them with paints possessing anticorrosion properties (Criado et al., 2015; Yang et al., 2015). Paints designed to protect metals against corrosion always contain corrosion-inhibiting pigments that slow down the metal corrosion process through electrochemical and chemical reactions (Ahmed et al., 2015; Vakili et al., 2015). Lead and chromium (VI) based pigments used to be routinely used in traditional oil paints, paints based on modified alkyd resins and other solvent-type paints (Patil & Radhakrishan, 2006). Roughly 30 to 40 years ago, efforts started to be made to remove toxic materials from workplaces and the environment, including toxic substances serving as pigments in corrosion protection paints. Although less environmentally harmful, current new anticorrosion pigments are less efficient than the traditional anticorrosion pigments (Granizo et al., 2013). Therefore, the possibility of developing nontoxic pigments for anticorrosion pigments that would feature efficiency at the same or even better level than the traditional toxic anticorrosion pigments is being explored. The potential of inorganic chemistry to offer suitable efficient non-toxic anticorrosion ingredients are currently virtually exhausted (Deya et al., 2002). A number of papers have been devoted to protective coatings containing pigments based on mixed oxides possessing the perovskite structure, which exhibit anticorrosion properties.

Electrochemically acting anticorrosion pigments passivate the substrate metal protected by the layer of the organic coating, acting either in the anodic region or in the cathodic region. Chemically and electrochemically acting pigments encompass a wide range of substances of various chemical composition, mainly lead-containing compounds and chromate pigments, phosphate compounds, modified phosphates, and metal powder based pigments. Paints with high zinc metal concentrations are routinely used (Naderi et al., 2014; Kalendová, 2000, 2003; Vliet, 1998).

Conductive polymers start to be popular among organic corrosion inhibitors (Armelin et al., 2009). Examples of conductive polymers include polypyrrole and polyaniline, involving systems of conjugated double bonds with the presence of charge carriers making possible charge transfer along the chain (Armelin et al., 2008). Owing to their properties, conductive polymers induce passivation processes on steel surfaces, in which respect they are similar to

the compounds containing heavy metals. This shows promise are regards the feasibility of using conductive polymers to replace, or reduce the use of, e.g., chromate-based corrosion inhibitors (Sangaj & Malshe, 2004). They may also find application as electrochemical, or electrically active, pigments to attain passivation of the surface of a corroding steel substrate (Lu et al., 1995; Wessling & Posdorfer, 1999).

Conductive polymers are used in protective organic coatings either on their own or together with other materials exhibiting anticorrosion effects or in the form of functional coatings on particles (Fig. 1) of the pigments (Grgur et al., 2015; Brodinová et al., 2007).

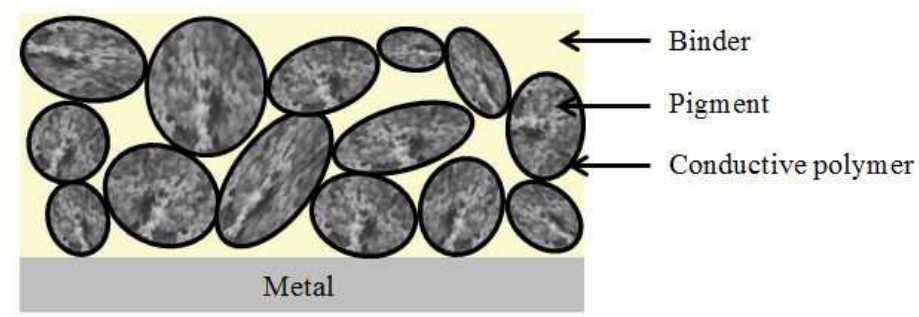

Fig. 1. Pigments treated conductive polymers on the surface layer.

A number of studies are under way examining the active effect of conductive polymers, e.g. polyaniline or polypyrrole, against metal corrosion if present in organic coatings (paints) as corrosion inhibitors. Inorganic pigments deliberately coated with a thin layer of polyaniline are used in some of them. The goal of those studies is to set up a new composite anticorrosion pigment that will provide a really high corrosion protection to the metal surface. In other words, a system is sought where the active anticorrosion effect comes both from the conductive polymer forming a thin layer on the pigment particle and from the pigment particle (core) itself. The core should contribute favourable physical properties of the paint and facilitate the corrosion-inhibiting function of the layer of the conductive polymer, e.g. polyaniline. Ideally, this layer should react to changes in the pH level and be transformed to the conductive form (Grgur et al., 2015; Brodinová et al., 2007; Mostafaei, 2014; Navarchian, 2014). In view of the specific properties of the paint binder and the different corrosion conditions, pigments must be sought whose physico-chemical properties will not affect adversely the stability of the film-forming component of the binder or the physical properties of the crosslinked polymeric coating (paint). The pigment surface is not covered by the conductive polymer completely, and so the two components-the pigment itself and the layer-act in concert. Largely, the preparatory process is conducted so that the degree of pigment particle coverage with polyaniline is 50–60 %.

Polyaniline phosphate is frequently used to coat the pigment particles; the phosphate ions from the acid (H_3PO_4) are not expected to have an unfavourable effect on the metal surface (Brodinová et al., 2007; Kalendová et al., 2008a).

Current research also focusses on the properties of pigments coated with layers of a conductive polymer, e.g. polyaniline, as potential anticorrosion pigments. If such inorganic carriers are identified as would assume the properties of the polymer, its conductive nature in particular, and ultimately would possess corrosion-inhibiting properties, they would be highly promising in the corrosion protection of metals. Conductive polymers are currently subject to extensive research in a number of sectors, among them the paint industry owing to their non-toxicity and high stability (Somboonsub et al, 2010; Király & Ronkay, 2015).

Composite particles consisting of an inorganic substance coated with a conductive polymer layer are advantageous ingredients of organic coating materials for active anticorrosion protection. Hence, they are pigment or filler particles that are provided with a layer of an active compound - an electrically conductive polymer. The core (chemically active pigment) should contribute the physical properties of the paint at the substrate metal-paint film interface, e.g. adhesion to the substrate, and ideally also provide additional active metal surface protection. In view of the specific properties of paint binders and of the various corrosion factors of the ambient environment, it is imperative to identify such a conductive modification type and volume concentration of the pigment/conductive polymer composite particles as do not affect adversely the stability of the film-forming component of the paint binder or the physical properties of the crosslinked polymeric coating material. The polymer must also retain its conductive form in order to continue to exert an anticorrosion protection effect. Therefore, “acid” binders, that is, binders containing, e.g., carboxy groups, such as alkyds, epoxy-esters and epoxy resins, are also suitable when using, e.g., polyaniline phosphate (PANI). In the specific case of PANI, such particles must not be appreciably alkaline, primarily in order to preserve the conductive form-emeraldine (Fig. 2) during polymerisation on the particle surface. No changes in the physical structure of the pigmented particles should occur during the preparation of the conductive polymer (Ahmed & MacDiarmid, 1996; Fang et al., 2007).

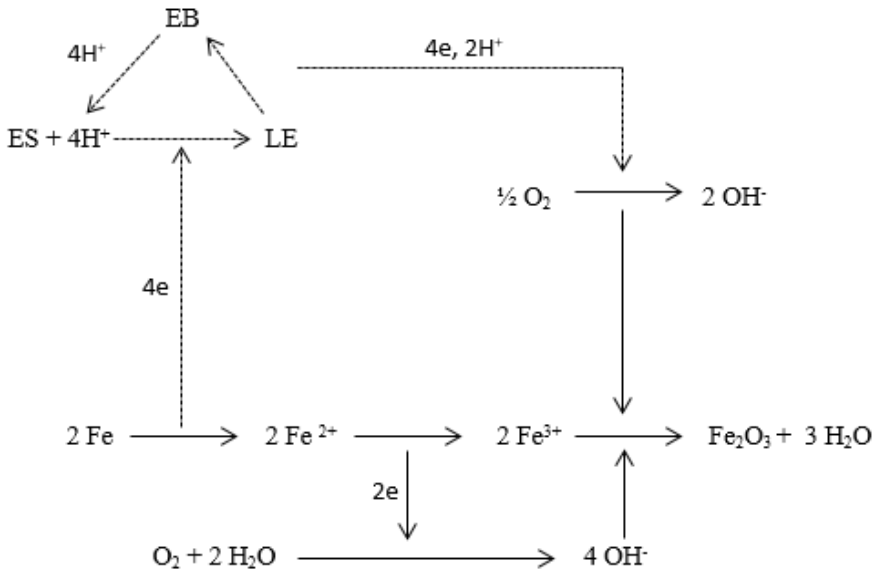

Fig. 2. Polyaniline forms and their interconversions (Wessling et al., 1996).

Study objectives

The perovskite type oxides, whose properties can be modified through the selection of the structural lattice-forming elements, were selected owing to the stability of their physical and chemical properties, insolubility, and thermal stability. In is also an asset of perovskites that they can be synthesized from a wide range of starting materials that are non-toxic and are reasonably environmentally friendly. The Ca^{2+} and Sr^{2+} cations were selected owing to their alkaline properties, which may be beneficial in suppressing corrosion of the metal surface beneath the paint film. The choice of those cations (Ca or Sr) in the perovskite structure (Fig. 3) can also be made use of to improve the inhibiting behaviour of the pigments, viz. through their rate or ease with which the cation can be released from the elementary lattice to act in the paint film. The perovskite carrier as well as the conductive polymer should modify the electric conductivity of the composite pigment particles and affect favourably the properties of the paint film when hindering electrochemical corrosion in environments with enhanced humidity/moisture, acid-nature corrosive substances and corrosion initiators. If the perovskites prove to be good carriers for the conductive polymer layers (pigment/conductive polymer system), they may open up the door to additional interesting applications-of the pigments as well as of the conductive polymers.

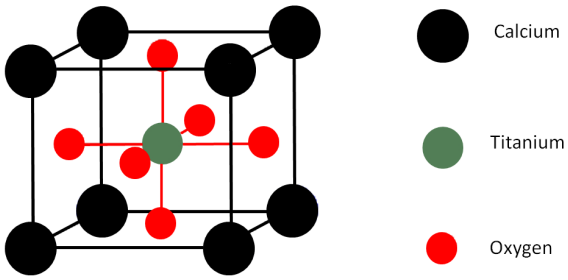

Fig. 3. The perovskite structure is named after the mineral $CaTiO_3$ (Kalendová *et al.*, 2014b).

The objectives of this study also included identification of the optimum pigment volume concentration (PVC) from two aspects: physical resistance of the paints containing the composite pigments under study and, in particular, their anticorrosion properties. The most efficient concentration may depend on the conductive polymer, perovskite structure and composition, and on the corrosive environment acting on the paint/metal system.

Experimental

Laboratory preparation of pigments

Perovskites with a generally isometric particle (Feng et al., 2008; Choudhary et al., 2000) shape were synthesized to serve as the pigment cores for coating with a conductive polymers and to be added to a binder to form anticorrosion paints. Pigments possessing the simple perovskite structure: $CaTiO_3$, $SrTiO_3$, $CaMnO_3$ and $SrMnO_3$, were synthesized by calcination.

The starting materials for the preparation of the pigments were as follows: titanium oxide (Precheza Přerov, a.s, CZ, composition: TiO_2 anatase); calcium carbonate (Omya a.s., Austria, composition: $CaCO_3$, natural calcite); strontium carbonate (Sigma-Aldrich Chemie, Germany, composition: $SrCO_3$); manganese (III) oxide (Sigma-Aldrich Chemie, Germany, composition: Mn_2O_3).

Pigment preparation procedure

The pigments were synthesized by solid-phase reaction, viz. by high-temperature calcination of the homogenized mixtures of the starting materials (Trojan et al., 1987) by following the general principles of preparation of high-temperature inorganic pigments (Alizahed et al., 2009). The process of preparing the pigments consists of 4 operational steps: homogenization of starting compound mixtures, calcination procedure leaching the calcination products by washing with water, and adapting the product to obtain the size of particles as

necessary by a wet grinding process. The process was conducted as a two-stage procedure: the pigments were first calcined at 1000 °C for 2 hours and then at 1180 °C. Since a suitable size of the pigment particles is a very important factor, the calcination step was followed by wet milling, performed in a Pulverisette 6 planetary ball mill (Netzsch, Germany). The pigment powder was placed in a milling container made from zircon-silicate ceramics and milled with rollers made from the corundum ceramics. The rotation speed was 400 rpm and the process was conducted for 4–5 hours. The milled pigments were rinsed with water again and at 105 °C in a laboratory electrical dryer.

Specification of the pigments

The structure of the perovskites was examined by X-ray diffraction analysis (XRD). The results gave evidence that the required structure had been attained. ABO_3 was found to be the majority phase in most of the pigments. Traces of the starting substances were detected in some of the products (Figs. 4–5). Some of the pigments contained traces of the starting TiO_2 or of reaction by-products. The pigment $CaTiO_3$ contained the main crystalline phase of $CaTiO_3$ and a small amount of rutile (TiO_2), $Ca(OH)_2$, and $CaCO_3$; $SrTiO_3$ contained the $SrTiO_3$ crystalline phase by TiO_2 (rutile) and $Sr_3Ti_2O_7$; $CaMnO_3$ contained the $CaMnO_3$ crystalline phase; and $SrMnO_3$ contained the $SrMnO_3$ crystalline phase and a small amount of $CaMn_2O_4$. The results gave evidence that the pigments intended for surface modification with the conductive polymers had been obtained as intended, and are in agreement with previous studies (Kalendová et al., 2015a). The regular shape of the pigment particles was documented by SEM photographs (Figs. 6–9).

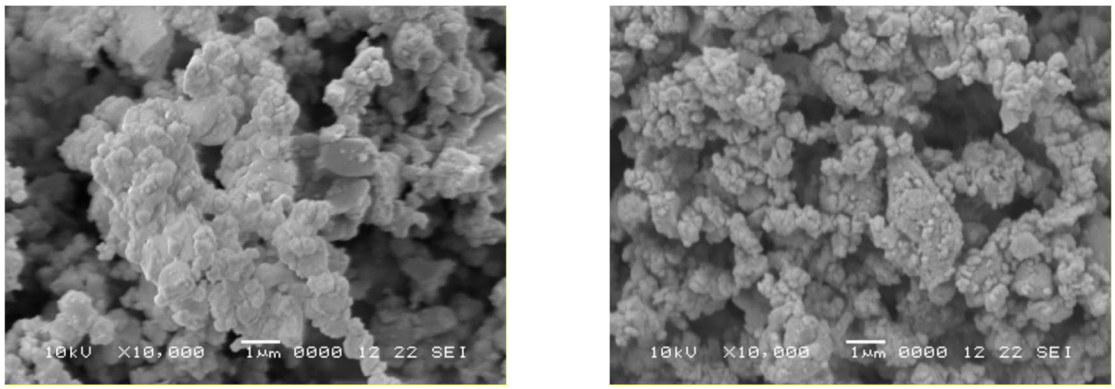

a) b)

Fig. 4. Morphology of perovskite particles as observed by SEM.
Notes: a) $CaTiO_3$ magnification 10000x; b) $SrTiO_3$ magnification 10000x.

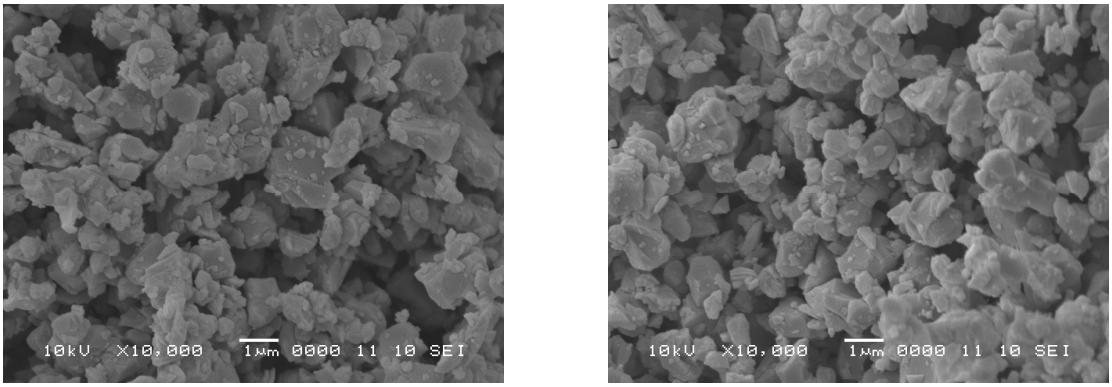

a) b)

Fig. 5. Morphology of perovskite particles as observed by SEM.
Notes: a) $SrMnO_3$ magnification 10000x; b) $CaMnO_3$ magnification 10000x.

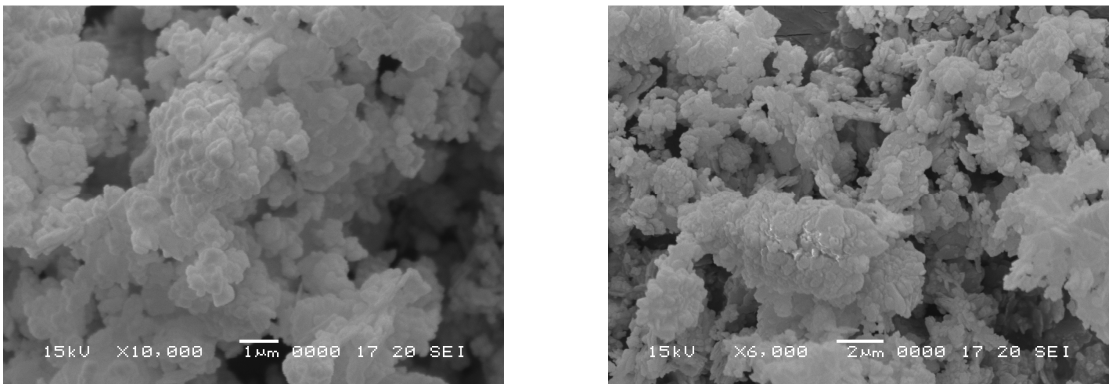

a) b)

Fig. 6. Morphology of perovskite particles with PANI and PPY as observed by SEM.
Notes: a) $CaTiO_3$/PANI magnification 10000x; b) $CaTiO_3$/PPY magnification 6000x.

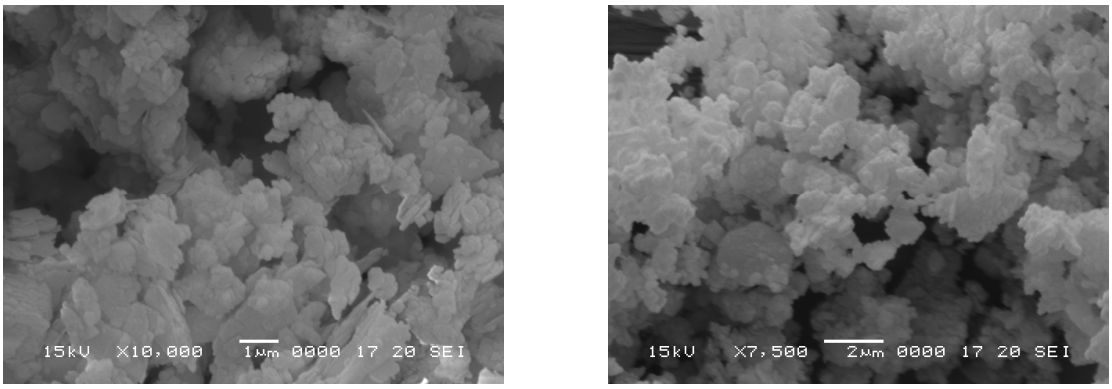

a) b)

Fig. 7. Morphology of perovskite particles with PANI and PPY as observed by SEM.
Notes: a) $SrTiO_3$/PANI magnification 10000x; b) $SrTiO_3$/PPY magnification 7500x.

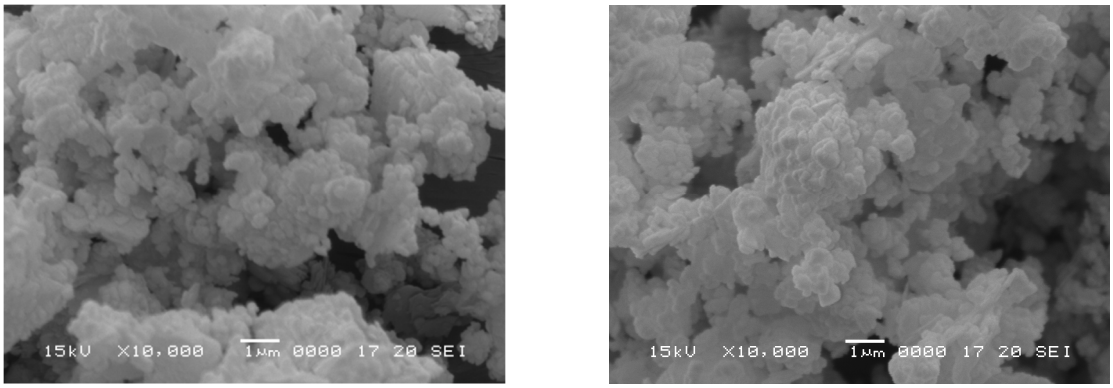

a) b)

Fig. 8. Morphology of perovskite particles with PANI and PPY as observed by SEM.
Notes: a) $SrMnO_3$/PANI magnification 10000x; b) $SrMnO_3$/PPY magnification 10000x.

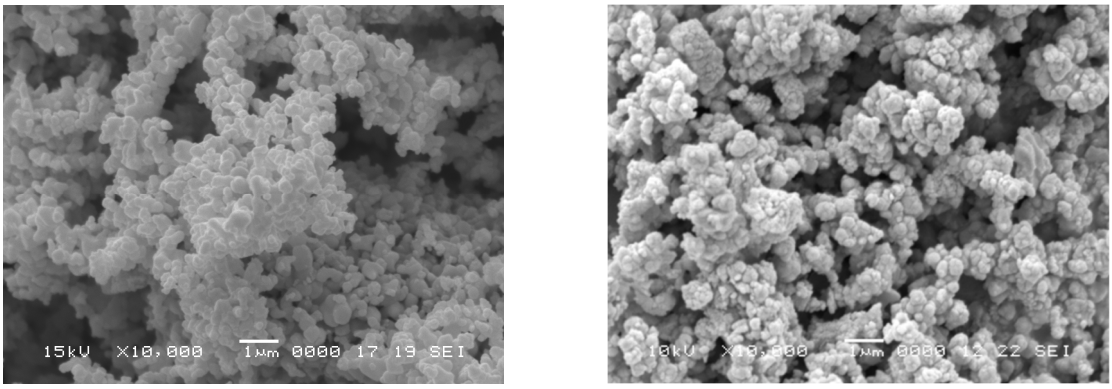

a) b)

Fig. 9. Morphology of perovskite particles with PANI and PPY as observed by SEM.
Notes: a) $CaMnO_3$ /PANI magnification 10000x; b) $CaMnO_3$/PPY magnification 10000x.

Physico-chemical properties of pigments

The basic physico-chemical properties of the inorganic pigments intended for surface modification with the conductive polymers were determined. The results are as follows.

$CaTiO_3$: density (4.120 g cm^{-1}), mean particle size d_{50} (0.829 µm), oil consumption (29.02 g 100 g^{-1}), CPVC (44 %), pH (12.48), specific electric conductivity (1850 µS cm^{-1}), water-soluble fraction (4.78 %); $SrTiO_3$: density (4.837 g cm^{-1}), mean particle size d_{50} (0.865 µm), oil consumption (26.25 g 100 g^{-1}), CPVC (42%), pH (10.16), specific electric conductivity (165.8 µS cm^{-1}), water-soluble fraction (0.82 %); $CaMnO_3$ density (4.281 g cm^{-1}), mean particle size d_{50} (3.924µm), oil consumption (21.47 g 100 g^{-1}), CPVC (50 %), pH (9.45), specific electric conductivity (78.3 µS cm^{-1}), water-soluble fraction (0.35 %); $SrMnO_3$ density (5.045 g cm^{-1}), mean particle size d_{50} (2.966 µm), oil consumption (20.08 g 100 g^{-1}), CPVC (48 %), pH (8.98), specific electric conductivity (206 µS cm^{-1}), water-soluble fraction (0.14 %).

Laboratory preparation of pigments with conductive polymer surface layers

The pigments: $CaTiO_3$, $SrTiO_3$, $CaMnO_3$, and $SrMnO_3$ were subjected to surface treatment with the conductive polymers with a view to optimising (enhancing) their anticorrosion properties.

Preparation of the perovskites modified with a surface layer of polyaniline phosphate (PANI)

The pigment (20 g) was suspended in 250 mL of 0.2 M aniline (C_6H_7N, Fluka, Switzerland) solution in 0.8 M *ortho*-phosphoric acid (Lachema, Czech Republic), and 250 mL

of 0.25 M ammonium peroxydisulfate (Lach-Ner, Czech Republic) also in 0.8 M *ortho*-phosphoric acid was added to initiate the aniline polymerization process at room temperature (Fig. 10). The suspension was stirred for one hour during which aniline polymerized on the surface of the pigment particles. Next day the solids were filtered out and rinsed with 0.4 M phosphoric acid followed by acetone. The pigment particles coated with the PANI overlayer were dried in air and then at 60 °C in a laboratory drier.

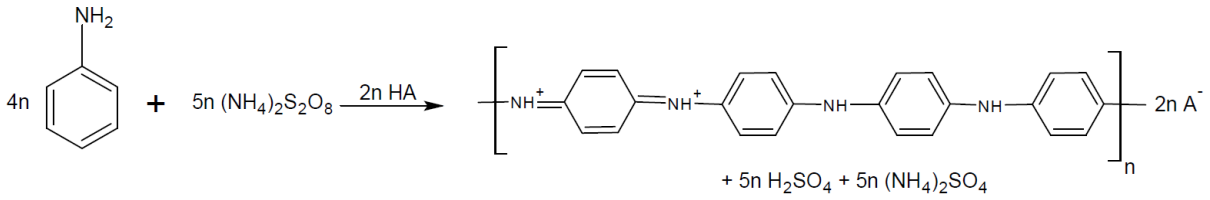

Fig. 10. Polymerisation of aniline.

Preparation of the perovskites modified with a surface layer of polypyrrole phosphate (PPY)

The pigment (20 g) was suspended in 250 mL of distilled water with 0.8 M *ortho*-phosphoric acid, (Lachema, Czech Republic), and 0.2 M pyrrole (C_4H_5N, Fluka, Sigma-Aldrich Co.) was added. The system was stirred vigorously by using a glass stirrer, and an oxidant solution consisting potassium 0.25 M peroxodisulfate (Lach-Ner, Czech Republic) in 250 mL of distilled water (Fig. 11) was added. The whole was stirred for approximately 1 hour. The next day the modified pigments were filtered out, rinsed with distilled water and acetone, and dried at room temperature in air and subsequently at 60 °C in a laboratory drier. The pigment particles coated with the PPY overlayer were dried in air and then at 60 °C in a laboratory drier.

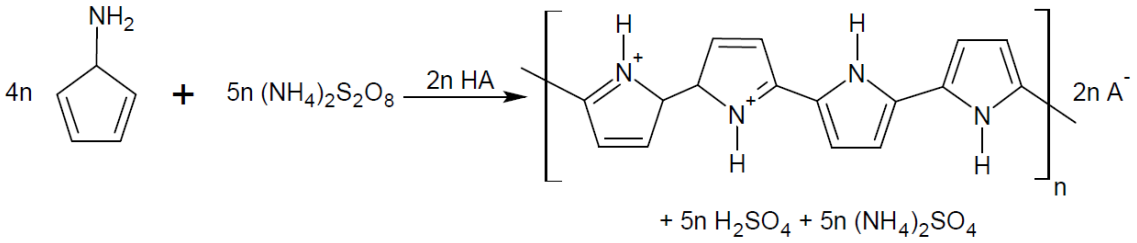

Fig. 11. Polymerisation of pyrrole.

Characterisation of the composite pigments containing a layer of a conductive polymer - PANI or PPY

The perovskite type pigments with their surfaces modified with PANI or PPY were prepared and subjected to X-ray fluorescence (XRF) analysis on a Philips PW 1404 X-ray

spectrometer equipped with a Rh cathode, in conjunction with UniQuant software enabling 74 elements (from fluorine to uranium) semiquantitatively determined (10 % relative error). X-ray diffraction spectra (XRD) of the synthetised perovskites were measured on an X'Pert PRO MPD 1880 X-ray diffractometer (PANanalytical, The Netherlands). The diffraction data were evaluated by means of the X´Pert programs (X´Pert HighScore Plus Software version 2.1 b and X´Pert Industry Software version 1.1 g); the phases were identified using data from the ICCD PDF2 diffraction database. The pigment surface and particle shape were examined on a JEOL-JSM 5600 LV scanning electron microscope (JEOL, Japan) in the secondary electron mode.

Determination of the physico-chemical properties of the pigments with conductive polymer surface layers

Determination of particle size and the distribution of pigment particle size were identified by means of Mastersizer 2000 (Malvern, Instruments Ltd., UK), which is able to measure the distribution of particles sizes from 0.01–2000 μm. Particle size is represented by the diameter of the equivalent sphere, i.e. sphere whose laser radiation dispersion patterns are identical with those of the particle in question. The pigments' specific weight was determined by using a AccuPyc II 1340, gas pycnometer (Micromeritics, USA. Linseed oil absorption was measured by the pestle-mortar method. The outcome, called the oil number (in g 100 g^{-1}), is a prerequisite for calculation of the CPVC and for the formulation of the paints Parameters are given as arithmetic averages within 10 measured values (Kalendová et al., 2009, 2010). The determination of the pH level of aqueous extracts of the pigments pH was based on the ISO 789-9 standard. 10 % pigment suspensions in redistilled water (pH = 7) were prepared and measured periodically during 28 days, after which they were filtered and the ultimate (constant) pH value of the filtrate (pH_p) , was recorded. A WTW 320 pH meter (WTW, Germany) served for the readings, and calibration buffers at pH = 4.01, 7.00, 10.01, and 12 at 25 °C were used. Specific electric conductivity of the 10 % pigment suspensions (χ_p) in redistilled water (specific electric conductivity 3 μS cm^{-1}) was also measured by means of a Handylab lF1 conductometer (SCHOTT, Germany) and calibration solutions whose specific electric conductivity was 37 μS cm^{-1} and 1413 μS cm^{-1} at 25 °C were used. This determination was based on the ISO 787-14 standard. The readings were made during 28 days and, like with the pH levels, the ultimate (constant) conductivity level was recorded. The pH values of aqueous extracts (pH_f) prepared from 10 % suspensions of loose paint films and the specific electric conductivity values of aqueous extracts (χ_f) prepared from suspensions of loose paint films at PVC = 1 %, 5 %, 10 %,

and 15 % were determined by the same method. The water-soluble fraction was measured gravimetrically by extraction of the powdered pigment, weighed with a precision of ± 0.01 g, in distilled water at 20 °C (W_{20}). This procedure was derived from the ČSN EN ISO 787-3 standard.

Formulation of the paints containing the pigments tested

Model solvent-based epoxy-ester resin-based paints were formulated for investigation of the pigments' anticorrosion properties. Description of binder: a 60 % solution of a medium high molecular weight epoxy resin esterified with a mixture of fatty acids of dehydrated ricin oil and soy oil, trade name WorléeDur D 46, acid number 4, viscosity 2.5–5.0 Pa s^{-1}, flow time (DIN 53211-4200) 250 s. The pigment volume concentration (PVC) in the paints were invariably 1, 5, 10 %, and 15 %. The PVC/CPVC ratio was adjusted in all the model paints to 0.50 by means of the anticorrosion-neutral filler calcite $CaCO_3$. The total pigment plus filler concentration in the paint film was 50 %, whereby a constant total concentration of the powder fractions in the dry paint film was assured, while varying only the proportion of the composite pigment. The paints were prepared by dispersing the powders in the liquid binder in a pearl mill Dispermat CV (WMA GETZMANN GmbH Verfahrenstechnik, Germany). Co-octoate in a fraction of 0.3 wt. % was used as the siccative.

Preparation of samples for the testing of the anticorrosion properties

Test samples were prepared by applying the paint to steel panels (deep-drawn cold-rolled steel, manufactured by Q-panel, UK) 150 mm × 100 mm × 0.9 mm size, by using a box-type application ruler with a 250 µm slot, modified as per ISO 1514. The dry film thickness (DFT) was measured with a Minitest 110 magnetic thickness gauge fitted with a F16 type probe (Elektrophysik, Germany) in accordance with ISO 2808 (Goldschmidt & Streitberger, 2007). A total of 10 test panels were prepared for each paint. A thin cut (groove) 7 cm long, which penetrated through the paint film and reached the substrate metal, was made by means of a sharp blade. The samples on the test panels were allowed to dry in standard conditions (temperature 20 °C, relative humidity 50 %) in a conditioned laboratory for 6 weeks. Paint films on polyethylene sheets were also prepared, peeled off when dry, and cut to pieces approximately 1 mm × 1 mm size. The unsupported films were used to prepare aqueous paint film suspensions in distilled water.

Cyclic corrosion test in an atmosphere with salt mist and condensing moisture

In this cyclic corrosion test the test panels were exposed to the mist of a 0.35 $(NH_4)_2SO_4$ + 0.05 wt. % NaCl solution at 35 °C ± 2 °C for 10 hours (1st cycle stage) and to condensing distilled water at 40 °C ± 2 °C for 1 hour (2nd cycle stage), followed by drying at 23 °C ± 2 °C (3rd cycle stage). The test encompassed 60 cycles, i.e. its total time was 1440 hours. The tests were conducted in a Liebisch S 400 salt chamber (Liebisch Labortechnik, Germany).

Corrosion test evaluation methods

After completing the corrosion tests the paints were evaluated by methods derived from the ASTM D 714-87, ASTM D 610, and ASTM D 1654-92 standards. Method classifies the osmotic blisters formed to groups defined by the sizes designated by 2, 4, 6 and 8 values (2 denoting the highest size, 8 the lowest size). To the blister size an information is attached giving the respective frequency of appearance. The highest frequency of appearance is designated as D (denoting dense), a lower one as MD (denoting medium denstity) and as F (denoting few). This approach can give a series starting with a surface showing the lowest corrosion attack by few osmotis blisters of small size up to dense large-size blisters. The corrosion phenomena evaluated included formation (size and frequency of occurrence) of blisters in the paint film surface and near a cut made in the film, percent fraction of substrate metal surface area affected by corrosion, and distance of propagation of substrate metal corrosion near the cut (in mm, both evaluated after removing the paint film). By connecting all the three (four) methods for the evaluation of various manifestations of the corrosion substrate attacts and of protective film alone we can obtain a single value of the protective efficiency. The results were converted to scores on a 100–0 scale, and a parameter called the overall anticorrosion efficiency of the paints was calculated by a mathematical relation (Veselý et al., 2010). The total anticorrosion efficiency from the cyclic corrosion tests was calculated as the arithmetic mean of the scores (Kalendová et al., 2010).

Linear polarisation

The linear polarisation method is applied to corrosion monitoring. It is designed specifically for the determination of the polarisation resistance R_p and current density I_{corr}. Linear polarisation was measured in a cell (Fig. 12) accommodating the reference electrode (saturated calomel electrode-SCE), counter-electrode (platinum electrode) and working

electrode constituted by the sample. The method is based on the fact that a linear segment near the corrosion potential occurs on the polarisation curve in linear coordinates.

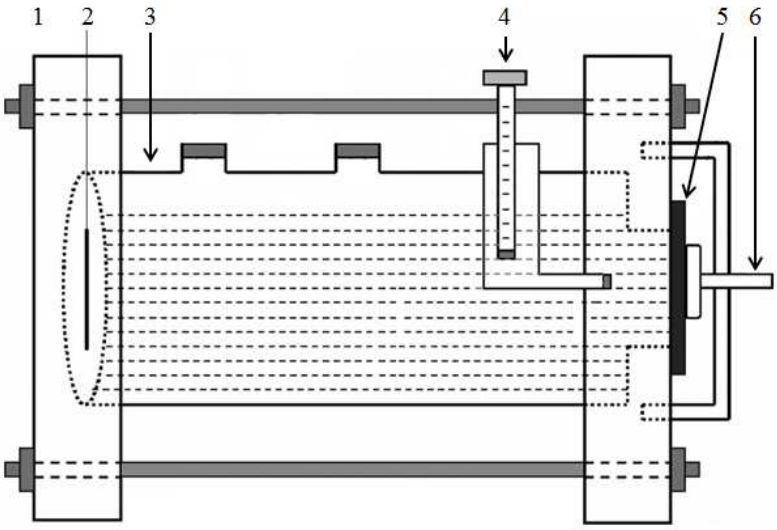

Fig. 12. Schematic diagram of the three-electrode experimental cell assembly (Kohl & Kalendová, 2014).

Notes: 1) PTFE board; 2) platinum counter electrode; 3) cylindrical glass reservoir (1 wt. % NaCl solution was placed in the glass reservoir); 4) reference electrode (saturated calomel electrode-SCE); 5) working electrode (steel panel with organic coating); 6) fixed bolt.

A 1 cm^2 area of the working electrode in the measuring cell was exposed to a 3.5 wt. % NaCl solution. The cell was connected to a potentiostat/galvanostat (VSP-300/France). The paint films were exposed to the NaCl solution for 24 hours, after which they were measured by the linear polarisation method. The polarisation region was from –10 mV/E_{OC} to +10 mV/E_{OC} at a rate of 0.166 mV s^{-1}. The following parameters were evaluated for each paint: spontaneous corrosion potential (E_{corr}), tafel region slopes (β_a and β_c), current density (I_{corr}), polarisation resistance (R_p), and corrosion rate (v_{corr}). Polarisation resistance R_p is defined as the inverse values of the current density I against the curve of the curve of the spontaneous corrosion potential E (at which $dE \rightarrow 0$). The polarisation resistance is defined by the relation in Eqs. (1) – (4) (Kouřil et al., 2006; Millard et al., 2001):

$$R_p = \frac{dE}{dI}, where\ dE \rightarrow 0 \quad (1)$$

$$I_{corr} = \frac{B}{R_p} \quad (2)$$

$$B_k = \frac{\beta_a\ \beta_c}{2.3\ (\beta_a + \beta_c)} \quad (3)$$

$$v_{corr} = \frac{I_{corr}\, M\, t}{\rho_{Fe}\, z\, F} \quad (4)$$

Effect of the pigments on the physico-mechanical properties of the organic coatings

The tests imitate mechanical stresses in the external environment, such as an object being dropped onto the surface (impact test) and deformations caused by bending and elongation (bending test and cupping test). Degree of adhesion of the paints was performed by the cross-cut test (ISO 2409). The lattice pattern was cut into the paint by means of a special cutting instrument with cutting blades that were 2 mm apart. The degree of adhesion of the 1 mm × 1 mm squares to the substrate was assessed. Impact resistance (ISO 6272) measured the maximum height of free drop of a weight (1000 g) at which the paint film still resisted damage. The test was performed by dropping the weight onto observe and reverse side of the test painted panel. Resistance of the paint film against cupping was made in an Erichsen cupping tester (ISO 1520). The objective of this test was to identify the resistance of the paint film against on-going deformation of a coated steel panel caused by indentation by a 20 mm steel ball. The cupping (in mm) giving rise to the first signs of disturbance of the paint film was measured. Resistance of the coating during bending over a cylindrical mandrel (ISO 1519) provided the largest diameter of the mandrel (in mm) causing disturbance of the paint film when the test panel is bent over it. The surface hardness of the paint film (ISO 1522) was determined by means of a pendulum according to Persoz. The results are indicated as per cents related to the hardness of glass standard (Goldschmidt & Streitberger, 2007).

Overall physico-mechanical resistance of the coatings

The results of the tests were used to calculate the overall physical-mechanical efficiency, i.e. overall paint film resistance to mechanical effects. A resistance score on the 100 - 0 scale (100 = excellent resistance, 0 = poor resistance) was assigned to each test result. The overall physical-mechanical resistance of the paints (*Me*) was calculated as the arithmetic mean of the three scores: the cohesion score from the bending test on the cylindrical mandrel, the resilience score from the impact test and the strength score from the cupping test (Veselý et al., 2012). The higher the Me score, the better the adhesion-barrier properties of the paint film.

Comparison experiments

The anticorrosion pigment based on the zinc phosphate hydrate $Zn_3(PO_4)_2 \times H_2O$ (PVC = 15 %) was also tested as a reference material allowing us to compare the results obtained with

the pigments synthesized by us with those obtained with a commercially available product. Films of the coating materials free from any pigment were also used in some tests, in the linear polarisation measurements.

Results and discussion

Structure and morphology of the composite pigment particles

Four perovskite type pigments were subjected to surface treatment with the conductive polymers PANI and PPY. Like the bare perovskite pigments, the pigments coated with the conductive polymers were subjected to X-ray diffraction (XRD) and X-ray fluorescence (XRF) analysis to elucidate their structure and composition. The results of the XRF data of the initial untreated pigments are listed in Table 1. The pigments contained Al_2O_3 in the order of tenths to units per cent (0.7–3.4 %) due to wear of the corundum milling bodies in the milling equipment. For the same reason the samples contained also trace amounts (0.11–0.41 %) of SiO_2. The two substances are neutral with respect to the chemical properties of the anticorrosion pigments. Analysis results (XRF) of surface treated pigments are given in Tables 2–3. The surface-modified (composite) pigments contained the respective oxides (TiO_2, Mn_2O_3, SrO, CaO), and also some amounts of compounds from the surface treatment procedure: P_2O_5 and SO_3 (associated with the polypyrrole phosphate/polyaniline phosphate layer). The surface treatment procedure was associated with weight loss of the oxides (of Ti, Mn, Ca, Sr) due to the nature of the medium (strongly acidic, with acids). What is important, however, is the fact that the pigment matrix for the conductive polymers and the mixed oxide contents were ensured (Tables 2–3). Once enveloped in a PANI or PPY layer, the oxides were protected from additional dissolution in an aqueous solution of phosphoric acid.

Structure analysis (XRD) results of surface treated pigments are given in Figs. 13–20 The composite pigments contained amorphous fractions of the conductive polymer and crystalline fractions of the carrier pigment. In addition of the amorphous fractions, which were invariably present, the composite pigments contained the following phases: $CaTiO_3$/PANI: a crystalline phase of $CaTiO_3$, a small amount of a by-phase of rutile (TiO_2) and $CaSO_4$; $CaTiO_3$/PPY: a crystalline phase of $CaTiO_3$, minor phases of rutile (TiO_2) and $CaSO_4$, and a small amount of anatase (TiO_2); $SrTiO_3$/PANI: a crystalline phase of $SrTiO_3$ and small amounts of rutile (TiO_2); $SrTiO_3$/PPY: a crystalline phase of $SrTiO_3$ and a small amount of $SrSO_4$; $CaMnO_3$/PANI: crystalline phases of $CaMnO_3$ and $CaSO_4$; $CaMnO_3$/PPY: a crystalline phase of $CaMnO_3$ and a smaller fraction of $CaSO_4$; $SrMnO_3$/PANI: a crystalline phase of $SrMnO_3$ and $SrSO_4$; and $SrMnO_3$/PPY: a crystalline phase of $SrMnO_3$ and a minor phase of $SrSO_4$. The

morphology of the composite pigments was examined by SEM. The pigment particle morphology is illustrated by scanning electron micrographs for the perovskites in Figs. 4–5, and for the surface modified perovskites in Figs. 6–9. The micrographs were taken in the secondary electron imaging (SEI) mode. The composite pigments had a tendency to form clusters.

Table 1. Results of XRF analysis of the untreated pigments (the data are in weight per cent; elements present at concentrations lower than 0.01 % are omitted)

Parameter/wt. %	$CaMnO_3$	$SrMnO_3$	$CaTiO_3$	$SrTiO_3$
Al_2O_3	3.00	0.70	3.20	3.40
SiO_2	0.25	0.16	0.41	0.11
CaO	43.61	-	39.44	-
MnO	53.14	57.72	-	-
SrO	-	41.42	-	52.98
TiO_2	-	-	56.95	43.51

Table 2. Results of XRF analysis of the treated pigments/PANI (the data are in weight per cent; elements present at concentrations lower than 0.01 % are omitted)

Parameter/wt. %	$CaTiO_3$/PANI	$SrTiO_3$/PANI	$CaMnO_3$/PANI	$SrMnO_3$/PANI
Al_2O_3	2.40	2.40	2.21	1.10
SiO_2	0.25	-	0.11	0.13
P_2O_5	9.50	10.70	8.20	17.80
SO_3	10.10	17.50	41.80	39.10
CaO	27.70	0.10	33.80	0.07
TiO_2	48.6	35.00	-	-
MnO	-	-	13.20	7.53
SrO	-	30.00	-	33.40

Table 3. Results of XRF analysis of the treated pigments/PPY (the data are in weight per cent; elements present at concentrations lower than 0.01 % are omitted)

Parameter/wt. %	$CaMnO_3$/PPY	$SrMnO_3$/PPY	$CaTiO_3$/PPY	$SrTiO_3$/PPY
Al_2O_3	2.20	1.30	2.35	2.10
SiO_2	0.12	0.18	0.13	-
P_2O_5	4.90	5.40	2.65	5.50
SO_3	37.2	42.70	16.90	11.5
CaO	34.1	0.08	29.70	0.12

TiO_2	-	-	46.80	42.8
ZnO	-	-	-	-
SrO	-	42.00	-	36.30
MnO	20.8	7.32	-	-

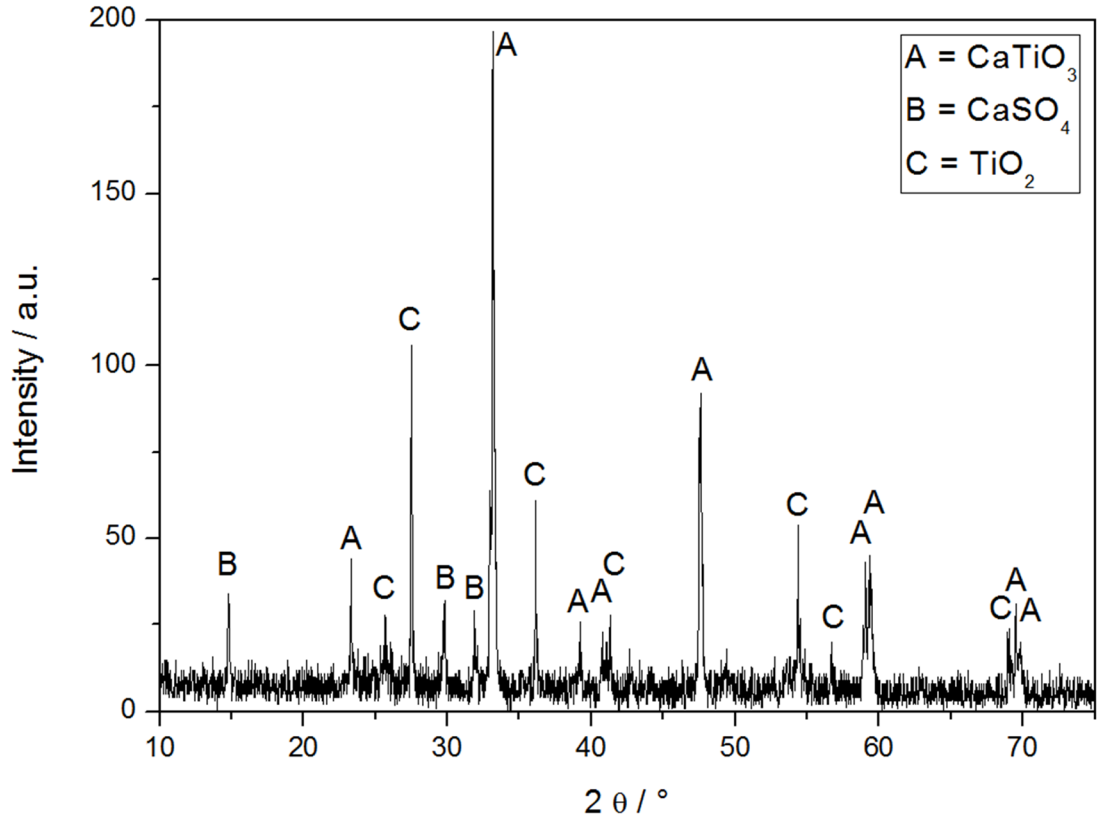

Fig. 13. Difractogram of the synthesised $CaTiO_3$/PANI.

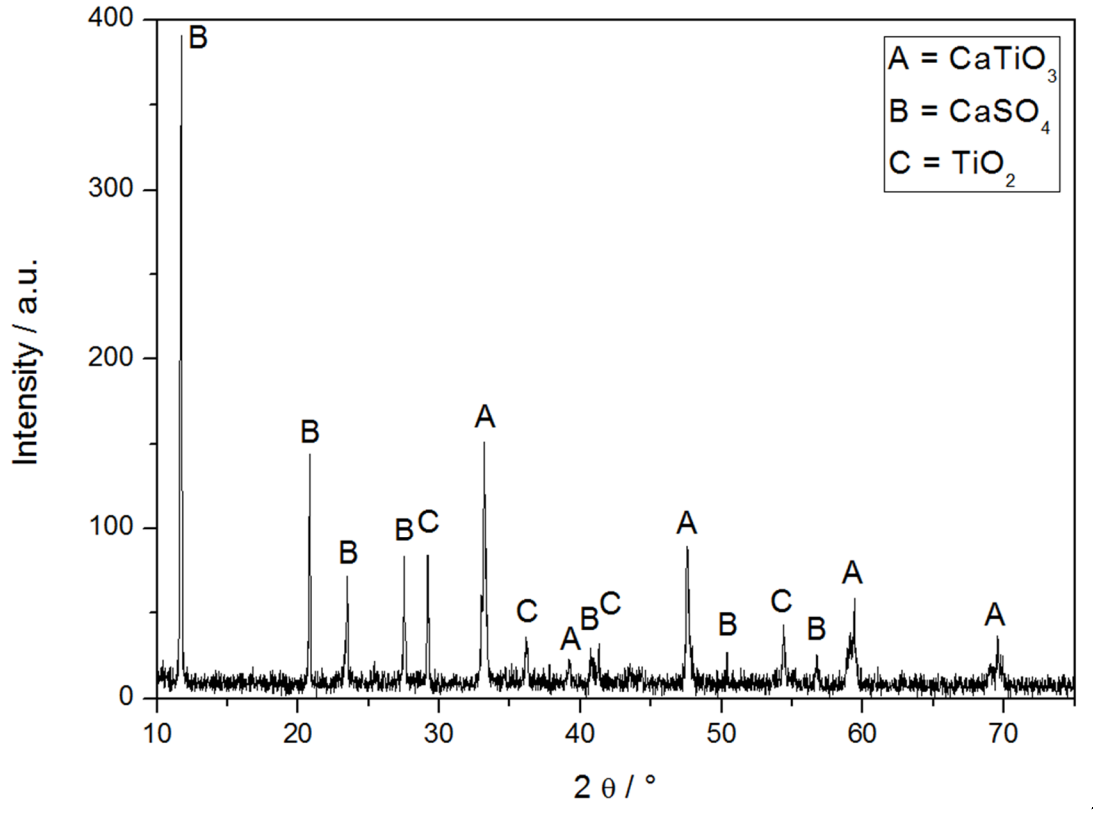

Fig. 14. Difractogram of the synthesised $CaTiO_3$/PPY.

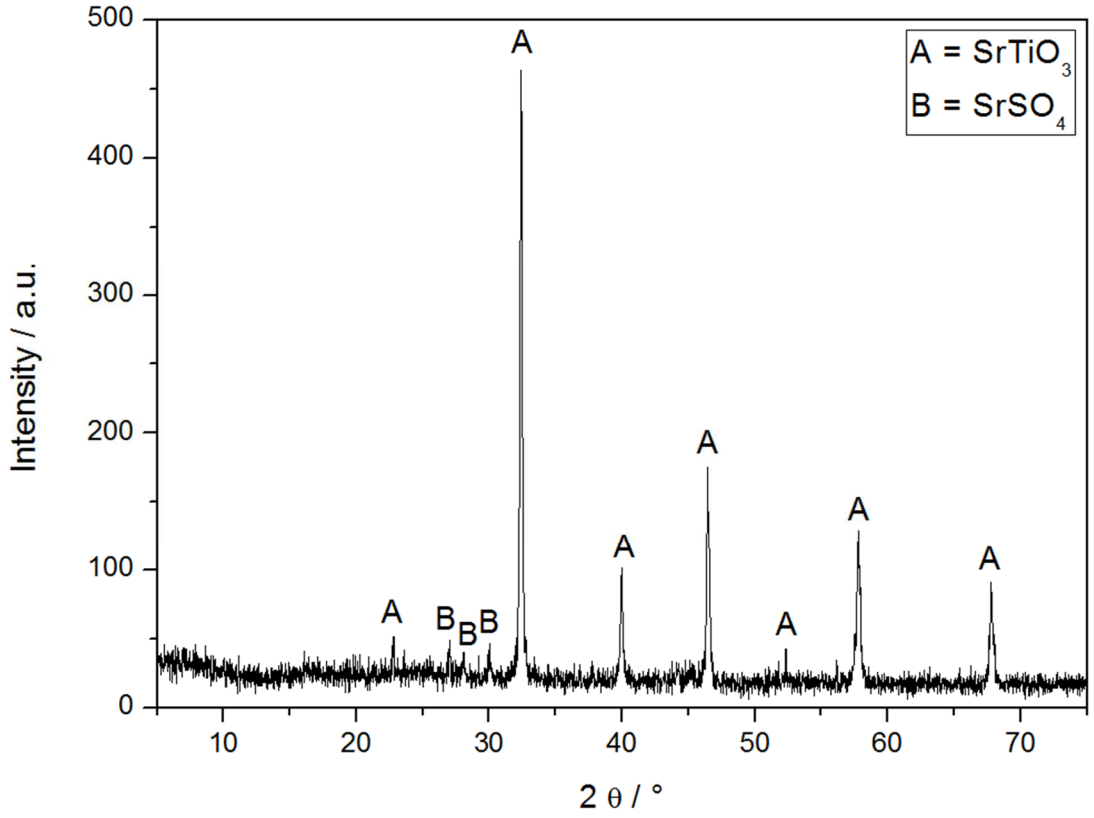

Fig. 15. Difractogram of the synthesised $SrTiO_3$/PANI.

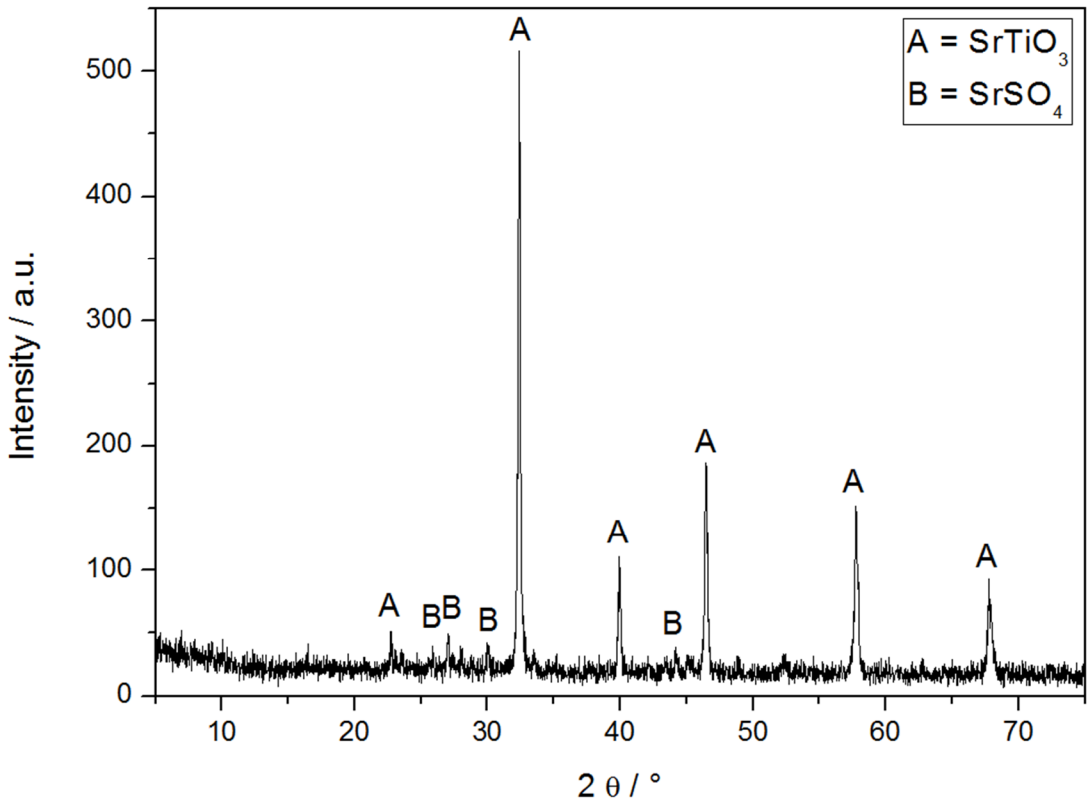

Fig. 16. Difractogram of the synthesised $SrTiO_3$/PPY.

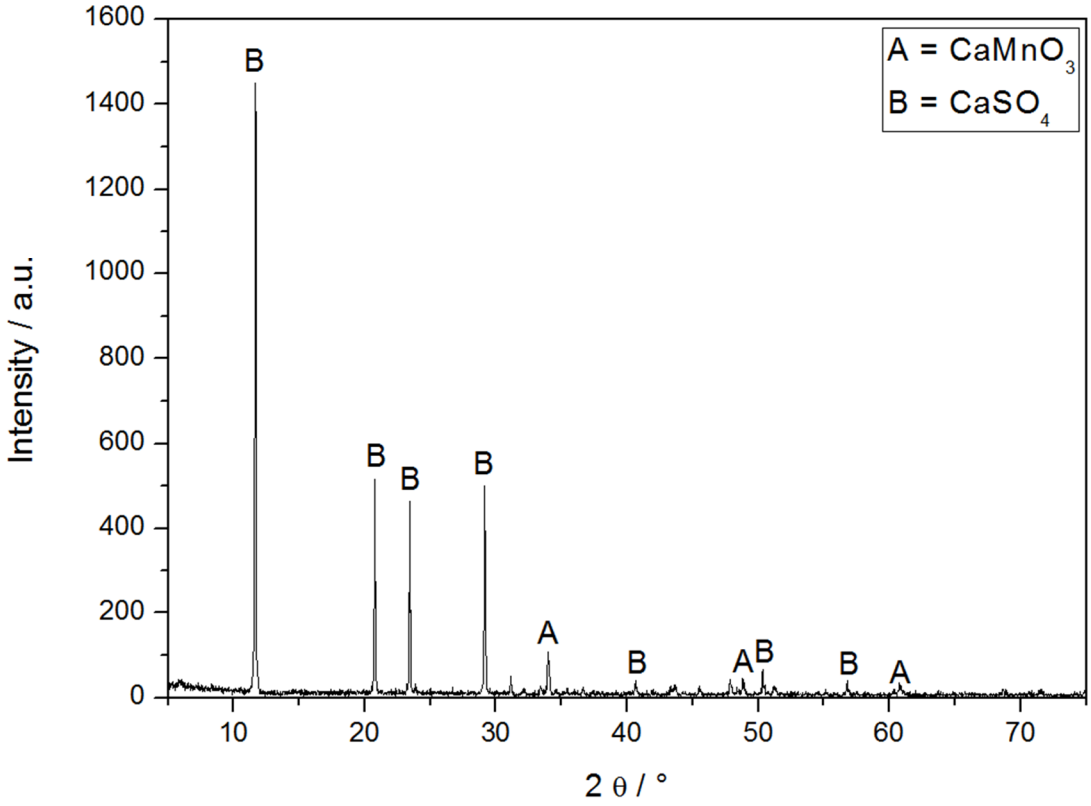

Fig. 17. Difractogram of the synthesised $CaMnO_3$/PANI.

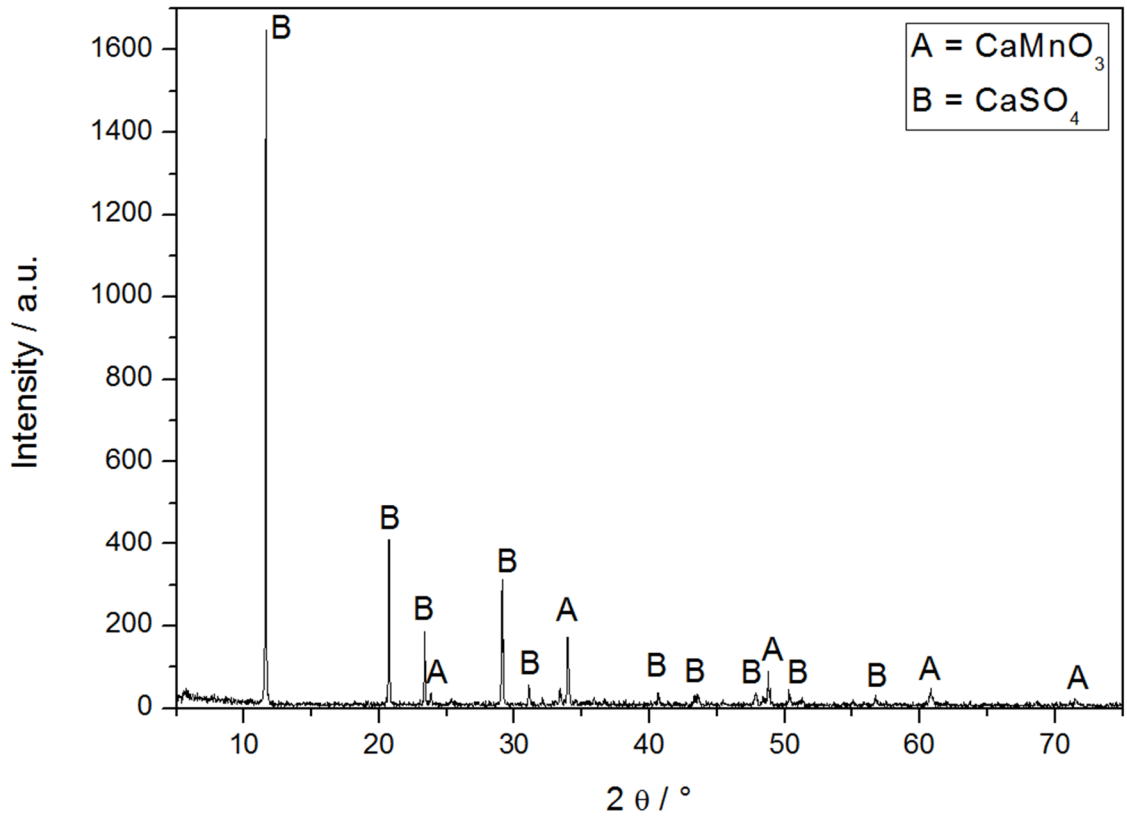

Fig. 18. Difractogram of the synthesised $CaMnO_3$/PPY.

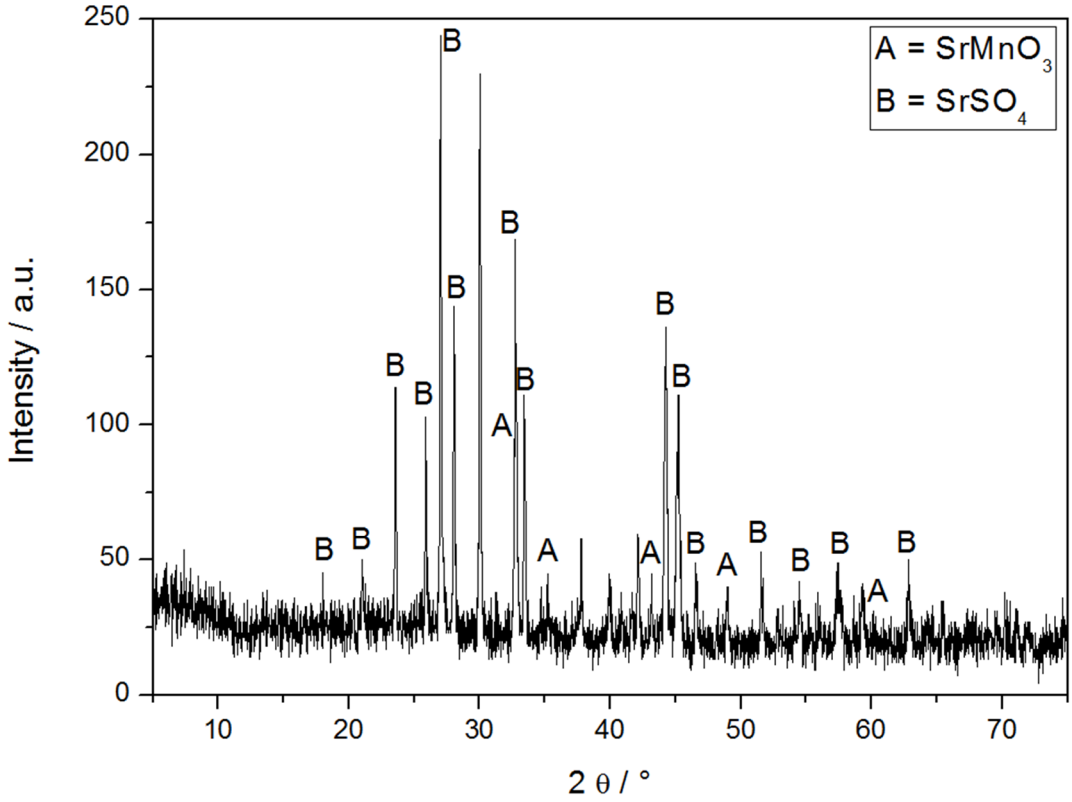

Fig. 19. Difractogram of the synthesised $SrMnO_3$/PANI.

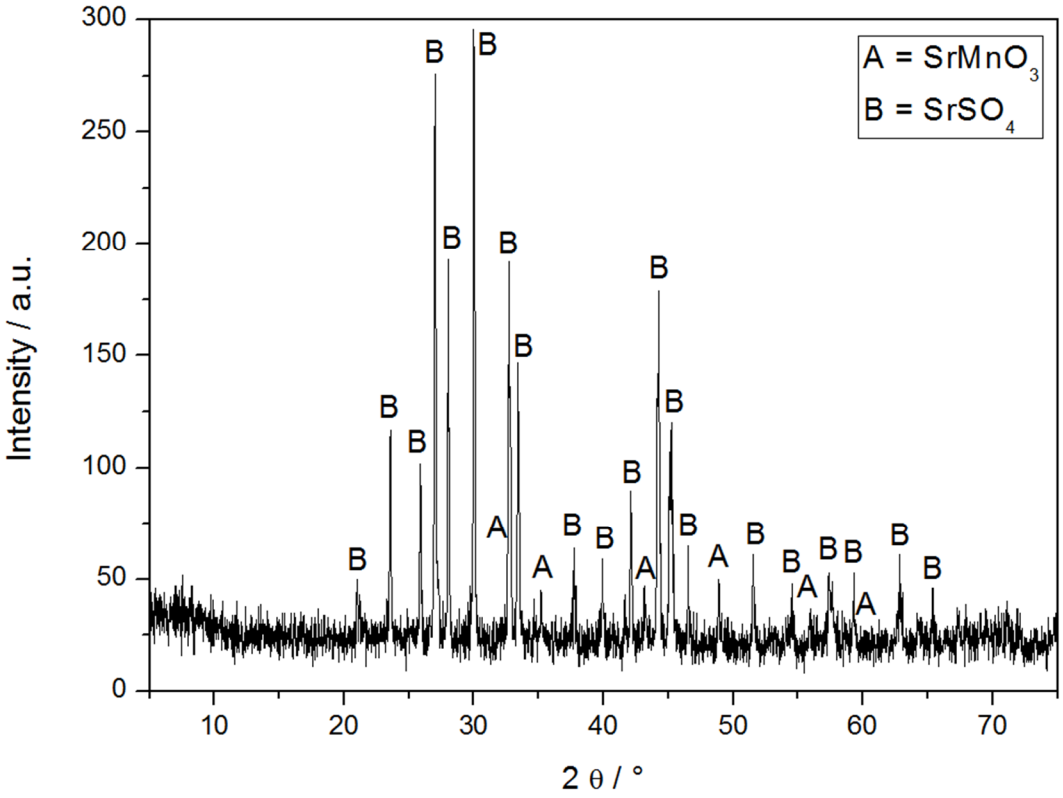

Fig. 20. Difractogram of the synthesised $SrMnO_3$/PPY.

Physico-chemical properties of the powdered pigments

The physico-chemical properties of the powdery pigments are given in Tables 4–5, including density, linseed oil consumption, CPVC, pH, specific electric conductivity, particle size distribution, and water-soluble fractions W_{20}. Table 5 lists the specific electric conductivities of the pigments in dependence on their concentrations in the paint films.

The densities of the perovskites coated with layers of PANI and of PPY lay within the ranges of 1.42–2.97 g cm^{-3} and 1.44–2.87 g cm^{-3}, respectively (Table 4), i.e. less than the densities of the initial inorganic perovskites. The densities of the PANI and PPY powders themselves are 1.58 g cm^{-3} and 1.76 g cm^{-3}, respectively (Kalendová et al., 2012b).

Oil consumption of the composite pigments with PANI and with PPY lay within the ranges of 37–57 g and 22–49 g per 100 g of the pigment, respectively (Table 4). The values were higher than those measured for the initial perovskite pigments due to the presence of the porous layers of the conductive polymers.. The oil consumption data for the composite pigments depended on the pigment particle heterodispersity; in fact, the oil consumption is generally dependent on the particle size and particle shape (i. e. on the specific surface area of the particle) (Kohl & Kalendová, 2014).

Knowledge of the critical pigment volume concentration CPVC value was a prerequisite for a correct formulation of a pigmented organic coating material (Kalendová & Veselý, 2009). The CPVC value depends on density and on the pigment's oil number. The critical pigment volume concentration levels were calculated to be about from 41 % to 80 % for the surface modified perovskites with PANI and from 50 % to 60 % for the perovskite pigments surface modified with PPY. From the above data it follows that the critical pigment volume concentrations (CPVC) of the composite pigments are lower for PANI than for PPY as the surface-modifying conductive polymer (Table 4).

Pigment surface modification with the conductive polymers shifted the pigment pH values to a more acidic region (Kalendová et al., 2008b). The pH level of the surface modified perovskites with PANI lay within the acidic region, attaining values from pH 3.0–5.6, whereas the surface perovskites with PPY were about pH 5.3–6.3 (Table 5). The pH values of the composite particles with PPY were more neutral than those of the composite particles with PANI.

The perovskite pigment surface treatment with the conductive polymers increased their specific electric conductivities. The specific electric conductivities were 2220 µS cm^{-1} for $CaTiO_3$/PANI and 2390 µS cm^{-1} for $CaTiO_3$/PPY; 1450 µS cm^{-1} for $SrTiO_3$/PANI and 1008 µS cm^{-1} for $SrTiO_3$/PPY; 2260 µS cm^{-1} for $CaMnO_3$/PANI and 2100 µS cm^{-1} for $CaMnO_3$/PPY; and 1024 µS cm^{-1} for $SrMnO_3$/PANI and 949 µS cm^{-1} for $SrMnO_3$/PPY. In summary, the specific conductivity ranges were similar for the two conductive polymers: 1024–2220 µS cm^{-1} for the pigments modified with PANI and 949–2390 µS cm^{-1} for the pigments modified with PPY. The carrier type did not affect the conductivity of the composite pigment as appreciably as the conductive polymer did. The specific conductivities of the PANI or PPY powders themselves were about 6940 µS cm^{-1} or up to 12600 µS cm^{-1} Kalendová et al., 2014a).

The electric conductivities of the composite pigments affected also the specific electric conductivities of the paint films pigmented with them (Table 6).

The cold water-soluble (W_{20}) fraction was from 5.09 % to 12.78 % for the pigments treated with PANI and from 3.36 % to 18.47 % for the pigments treated with PPY.

Table 4. Physico-chemical properties of the powdered pigments

Pigment	ρ/g cm^{-3}	oil abs/g $100g^{-1}$	CPVC/%
$CaTiO_3$/PANI	2.97	37	46
$SrTiO_3$/PANI	2.76	49	41

$CaMnO_3$/PANI	2.17	57	43
$SrMnO_3$/PANI	1.42	55	80
$CaTiO_3$/PPY	2.83	22	60
$SrTiO_3$/PPY	1.44	49	57
$CaMnO_3$/PPY	2.54	31	54
$SrMnO_3$/PPY	2.87	33	50
$Zn_3(PO_4)_3 \times H_2O$	3.28	34	45

Table 5. Physico-chemical properties of the pigments

Pigment / coating	Aqueous extracts of the pigments			Aqueous extracts of the paint films
	W_{20}/%	pH_p	χ_p/μS cm^{-1}	pH_f
$CaTiO_3$/PANI	9.46	4.34 ± 0.01	2220 ± 0.5 %	6.544 ± 0.01
$SrTiO_3$/PANI	5.09	3.00 ± 0.01	1450 ± 0.5 %	6.164 ± 0.01
$CaMnO_3$/PANI	12.78	5.62 ± 0.01	2260 ± 0.5 %	7.444 ± 0.01
$SrMnO_3$/PANI	9.78	5.03 ± 0.01	1024 ± 0.5 %	7.274 ± 0.01
$CaTiO_3$/PPY	10.69	5.29 ± 0.01	2390 ± 0.5 %	7.284 ± 0.01
$SrTiO_3$/PPY	10.07	6.02 ± 0.01	1008 ± 0.5 %	7.654 ± 0.01
$CaMnO_3$/PPY	18.47	6.26 ± 0.01	2100 ± 0.5 %	7.734 ± 0.01
$SrMnO_3$/PPY	3.36	6.17 ± 0.01	949 ± 0.5 %	7.464 ± 0.01
$Zn_3(PO_4)_3 \times H_2O$	0.26	6.65 ± 0.01	50 ± 0.5 %	7.284 ± 0.01
Non-pigmented film	-	-	-	3.714 ± 0.01

Table 6. Specific electric conductivity of aqueous extracts of loose paint films containing the composite pigments

Pigment modified with PANI	PVC/%	χ_f/μS cm^{-1}	Pigment modified with PPY	PVC/%	χ_f/μS cm^{-1}
$CaTiO_3$/PANI	1	313 ± 0.5 %	$CaTiO_3$/PPY	1	542 ± 0.5 %
	5	318 ± 0.5 %		5	584 ± 0.5 %
	10	348 ± 0.5 %		10	626 ± 0.5 %
	15	465 ± 0.5 %		15	992 ± 0.5 %
$SrTiO_3$/PANI	1	332 ± 0.5 %	$SrTiO_3$/PPY	1	446 ± 0.5 %
	5	431 ± 0.5 %		5	454 ± 0.5 %
	10	589 ± 0.5 %		10	461 ± 0.5 %
	15	778 ± 0.5 %		15	521 ± 0.5 %

$CaMnO_3$/PANI	1	381 ± 0.5 %	$CaMnO_3$/PPY	1	530 ± 0.5 %
	5	443 ± 0.5 %		5	645 ± 0.5 %
	10	1353 ± 0. 5%		10	887 ± 0.5 %
	15	1894 ± 0.5 %		15	1204 ± 0.5 %
$SrMnO_3$/PANI	1	364 ± 0.5 %	$SrMnO_3$/PPY	1	398 ± 0.5 %
	5	421 ± 0.5 %		5	503 ± 0.5 %
	10	513 ± 0.5 %		10	558 ± 0.5 %
	15	851 ± 0.5 %		15	639 ± 0.5 %
$Zn_3(PO_4)_3 \times H_2O$	15	176 ± 0.5 %	Non-pigmented film	-	50 ± 0.5 %

Corrosion tests

The size and frequency of blisters in the paint film were determined as per ASTM D 714-87, the fraction of substrate metal area affected by corrosion was determined as per ASTM D 610, the distance of propagation of corrosion in the cut was determined after removing the paint film as per ASTM D 1654-92, and the overall anticorrosion efficiency ($E_{electrol}$) was calculated as described above (Kalendová et al., 2010).

The results of the corrosion test of the paints with the pigments in the environment of NaCl and $(NH_4)_2SO_4$ mist and the calculated overall anticorrosion efficiency $E_{electrol}$ are given in Table 9.

Table 9. Results of accelerated corrosion tests of the paints containing composite pigments in mist of a salt electrolyte (exposure 1440 hours, DFT = 95 ± 10 μm)

Pigment	PVC/ %	Blistering		Corrosion		Anticorrosion efficiency $E_{electrol}$/%
		In a cut/ dg	Metal base/ dg	In the cut/ mm	Metal base/ %	
$CaTiO_3$/PANI	1	-	4MD	2.5–3.0	3	66
	5	-	6MD	2.0–2.5	10	68
	10	-	6M	2.0–2.5	>50	58
	15	-	6MD	2.0–2.5	50	53
$SrTiO_3$/PANI	1	2D	-	2.5–3.0	0.1	67
	5	-	4MD	2.5–3.0	0.1	73
	10	-	-	0	>50	76
	15	4M	8M	0.5–1.0	>50	50
$CaMnO_3$/PANI	1	2M	6MD	2.5–3.0	0.3	60
	5	2M	8M	3.0–4.0	10	58

	10	-	8MD	0.5–1.0	>50	58
	15	-	8MD	1.5–2.0	>50	55
$SrMnO_3$/PANI	1	4M	6MD	1.0–1.5	3	60
	5	2M	6MD	2.0–2.5	10	54
	10	2F	6MD	1.5–2.0	>50	45
	15	-	-	0.5–1.0	>50	73
$CaTiO_3$/PPY	1	2M	-	1.5–2.0	0.1	79
	5	4M	6M	1.0–1.5	0.3	71
	10	2M	6F	1.5–2.0	1	70
	15	4M	6M	1.0–1.5	>50	48
$SrTiO_3$/PPY	1	-	4M	2.5–3.0	0.03	79
	5	4M	6MD	0.5–1.0	0.03	68
	10	-	4MD	2.0–2.5	1	71
	15	2F	4D	1.5–2.0	1	59
$CaMnO_3$/PPY	1	2M	4M	3.0–4.0	1	60
	5	2M	4M	3.0–4.0	50	40
	10	2M	4M	2.5–3.0	>50	41
	15	2M	6MD	2.5–3.0	>50	38
$SrMnO_3$/PPY	1	-	6M	0.5–1.0	0.3	84
	5	-	6F	0–0.5	0.1	92
	10	-	6M	0–0.5	16	74
	15	4M	4M	1.0–1.5	33	53
$Zn_3(PO_4)_3 \times H_2O$	15	2M	8M	4.0–5.0	10	59
Non-pigmented film	-	-	-	0.5–1.0	>50	73

Linear polarisation

The results of the electrochemical linear polarisation measurements of the paints are listed in Table 10. The measurements provided values of the spontaneous corrosion potential, polarisation resistance, and corrosion rate of the paint films, from which information of the paint film resistance to corrosion can be derived. The spontaneous corrosion potentials (E_{corr}) of the paints containing the pigments modified with the conductive polymers at PVC = 1–15 % lay within the regions from −687 to −286 mV for PANI and from −600 to −120 mV for PPY, the corresponding polarisation resistance (R_p) ranges were from 1×10^5 to 7×10^7 Ω for PANI

and from 2×10^5 to 7×10^{10} Ω for PPY. The corrosion rates (v_{corr}) lay within the regions from 8×10^{-7} to 2×10^{-4} mm/year for the paints with the pigments modified with PANI and from 1×10^{-11} to 4×10^{-4} mm/year for the paints with the pigments modified with PPY.

Table 10. Results of linear polarisation measurements of the paints containing composite pigments, DFT = 60 ± 10 μm

Pigment in the paint	PVC/%	E_{corr}/mV	I_{corr} /μA	R_p/Ω	v_{corr}/mm year^{-1}
$CaTiO_3$/PANI	1	−431	7×10^{-4}	1×10^{7}	8×10^{-7}
	5	−382	2×10^{-4}	2×10^{7}	1×10^{-5}
	10	−463	4×10^{-3}	2×10^{6}	5×10^{-4}
	15	−468	8×10^{-3}	7×10^{5}	8×10^{-4}
$SrTiO_3$/PANI	1	−286	7×10^{-4}	5×10^{7}	8×10^{-7}
	5	−593	1×10^{-3}	4×10^{6}	1×10^{-5}
	10	−587	5×10^{-2}	1×10^{5}	5×10^{-4}
	15	−635	7×10^{-2}	1×10^{5}	8×10^{-4}
$CaMnO_3$/PANI	1	−687	9×10^{-5}	7×10^{7}	1×10^{-6}
	5	−558	7×10^{-3}	1×10^{6}	8×10^{-5}
	10	554	1×10^{-3}	2×10^{6}	1×10^{-5}
	15	−563	3×10^{-2}	2×10^{5}	4×10^{-4}
$SrMnO_3$/PANI	1	−585	3×10^{-3}	2×10^{6}	3×10^{-5}
	5	−551	4×10^{-3}	2×10^{6}	5×10^{-5}
	10	−590	2×10^{-2}	3×10^{5}	2×10^{-4}
	15	−651	6×10^{-3}	6×10^{5}	7×10^{-5}
$CaTiO_3$/PPY	1	−175	1×10^{-7}	5×10^{10}	1×10^{-11}
	5	−192	4×10^{-7}	3×10^{9}	5×10^{-9}
	10	−354	2×10^{-6}	4×10^{9}	2×10^{-8}
	15	−600	8×10^{-4}	1×10^{7}	9×10^{-6}
$SrTiO_3$/PPY	1	−556	7×10^{-8}	7×10^{10}	8×10^{-10}
	5	−553	5×10^{-8}	4×10^{10}	6×10^{-10}
	10	−544	4×10^{-4}	2×10^{7}	4×10^{-6}
	15	−521	3×10^{-4}	2×10^{7}	5×10^{-6}
$CaMnO_3$/PPY	1	−120	6×10^{-8}	4×10^{10}	7×10^{-10}
	5	−372	1×10^{-3}	6×10^{6}	1×10^{-5}
	10	−483	8×10^{-3}	7×10^{5}	9×10^{-5}
	15	−576	3×10^{-2}	2×10^{5}	4×10^{-4}
$SrMnO_3$/PPY	1	−574	6×10^{-6}	7×10^{8}	7×10^{-7}
	5	−500	2×10^{-6}	3×10^{9}	2×10^{-8}

	10	−492	2×10^{-3}	2×10^{6}	2×10^{-5}
	15	−509	4×10^{-4}	8×10^{6}	5×10^{-6}
$Zn_3(PO_4)_3\times H_2O$	15	−473	1×10^{-4}	3×10^{7}	1×10^{-6}
Non-pigmented film	0	42	2×10^{-3}	3×10^{6}	1×10^{-5}

Effect of the pigments on the physical properties of the paint films

The data of physical properties of the paint films with the pigments are given in Table 11.

Table 11. Physico-mechanical parameters of the paint containing composite pigments (DFT = 60 ± 10 μm)

Pigment in the paint	PVC/ %	Cupping/ mm	Adhesion/ dg	Impact		Bending /mm	Overall mechanical resistance/%
				Insight side/cm	Reverse side/cm		
$CaTiO_3$/PANI	1	>10	0	100	<10	4	86
	5	>10	0	100	50	4	93
	10	>10	0	100	100	4	100
	15	>10	0	100	40	4	91
$SrTiO_3$/PANI	1	>10	0	100	30	4	72
	5	9.8	0	100	70	4	97
	10	9.7	0	100	100	4	100
	15	9.1	0	100	100	4	99
$CaMnO_3$/PANI	1	8.9	0	100	<10	4	65
	5	>10	0	100	40	4	71
	10	5.9	0	100	100	4	95
	15	9.7	0	100	100	4	100
$SrMnO_3$/PANI	1	9.8	0	100	10	4	86
	5	>10	0	100	20	4	86
	10	>10	0	100	60	4	95
	15	9.7	0	100	100	4	100
$CaTiO_3$/PPY	1	5.3	0	100	<10	8	79
	5	9.5	0	100	20	4	85
	10	8.9	0	100	60	4	94
	15	8.3	0	100	100	4	98
$SrTiO_3$/PPY	1	8.9	0	100	60	4	94
	5	9.1	0	100	90	4	98
	10	>10	0	100	100	4	100
	15	>10	0	100	100	4	100
$CaMnO_3$/PPY	1	-	0	100	<10	10	60

	5	-	0	100	50	4	92
	10	-	0	100	80	4	97
	15	-	0	100	100	4	99
$SrMnO_3$/PPY	1	-	0	100	<10	6	75
	5	-	0	100	<10	4	83
	10	-	0	100	85	4	98
	15	-	0	100	90	4	98
$Zn_3(PO_4)_3 \times H_2O$	15	>10	0	100	10	4	83
Non-pigmented film	-	>10	0	>100	>100	>4	100

Results and discussion

Structure of the composite pigments, particle morphology

A total of 8 pigments surface modified with the conductive polymers PANI and PPY were prepared for testing in protective coatings. The composite pigments contained an amorphous fraction of the conductive polymer and a crystalline fraction of the perovskite carrier (Figs. 4–5), i.e. $CaTiO_3$, $SrTiO_3$, $CaMnO_3$, and $SrMnO_3$, sometimes by lower amounts of the unreacted starting materials or products formed during the pigment surface treatment with the conductive polymers ($CaSO_4$, $SrSO_4$, rutile, anatase both are TiO_2 species). The particles of the initial perovskite pigments had a regular nodular shape (Fig. 3), which remained unaffected by surface treatment (Figs. 6–8). The particles of the pigments modified with the conductive polymers agglomerated into clusters (Kohl & Kalendová, 2014).

Water-soluble contents

The water-soluble contents (W_{20}) of the pigments are listed in Table 5. The water soluble content was higher in the pigments modified with the conductive polymers than in the initial inorganic perovskites due to the presence of minor by-phases such as $CaSO_4$ or $SrSO_4$. The lowest content of substances soluble in cold water, W_{20} = 3.36 %, was found in the $SrMnO_3$/PPY system, the highest content, W_{20} = 18.47 %, in the $CaMnO_3$/PPY system due to the presence of the by-phase of $CaSO_4$. The differences in the water-soluble contents between the pigments coated with PPY and the pigments coated with PANI were units per cent only: e.g., the maximum value observed with PPY was W_{20}=18.47 % and the maximum value observed with PANI was W_{20} = 12.78 %. The increased water soluble content of the modified pigments compared to the non-modified pigments also supports the concept of deprotonation of the

conductive polymer layers in the former (Kohl & Kalendová, 2014). A high water-soluble content in indicative of a potentially increased occurrence of osmotic blisters on the surfaces of the paint films (Kalendová et al., 2015b). It is concluded that the pigments are not “hazardous” because of this parameter (Kalendová et al., 2014a).

pH values of aqueous extracts of the pigments and of loose paint films

The observed pH values of the pigment powders (pH_p) and of loose paint films containing the pigments (pH_f) are listed in Table 5. The values of extracts of the non-modified perovskite pigments lay with the region of pH 9–12, the values of extracts of the pigments coated with the conductive polymer layers lay within the range of pH_p 3.0–6.3. Hence, the pigment surface treatment brought about pH shift towards more acid values: modification with PPY shifted the pH to a slightly acidic region, modification with PANI, to the acid region. This shift can be explained in terms of deprotonation of the phosphate salts of PANI/PPY in aqueous solutions. The presence of the PANI or PPY salt in the composite pigment reduced the individual differences in the pH values between the initial perovskites.

The pH_f values of extracts of the loose pigmented paint films lay within the region of pH_f 6.2–7.7; within this region, the paint films containing PPY occupied the basic side (pH_f 7.3–7.7); within this region, the paint films containing PANI occupied the basic side (pH_f 6.2 – 7.4). The pH of the extract of the non-pigmented film lay in the acid region, at pH 3.7. The pH values for the paints containing the composite pigments were also affected by the presence of $CaCO_3$ in the paint, or by release of the basically reacting calcium and strontium cations (Ca^{2+}, Sr^{2+}). The pH of the extract of the paint film containing calcite at PVC = 50 % lay in the slightly basic region, at pH 8.47. This is beneficial with respect to suppression of corrosion on the metal surface beneath the paint film.

Specific conductivities of aqueous extracts of the pigments and of the loose paint films

Some electric conductivity is necessary for the anticorrosion pigments to passivate the metal surface beneath the paint film. The specific conductivities of extracts of the pigment powders modified with the conductive polymers lay within the regions of 949–2390 μS cm^{-1} for PPY and 1024–2260 μS cm^{-1} for PANI and increased in time due to the release of the soluble components into the aqueous environment. The specific electric conductivities did not differ appreciably between the individual surface-modified pigments: the differences lay within one order of magnitude - from 2390 μS cm^{-1} to 949 μS cm^{-1}. Hence, the specific conductivity was

one to two orders of magnitude higher for the composite pigments than for the initial perovskites.

The specific conductivity of the aqueous extracts of the loose films (χ_f) increased with increasing conductive polymer content of the paint (Table 6). The specific conductivities were lowest for the paints with PVC = 1 %, from 313 μS cm^{-1} to 381 μS cm^{-1}. For the pigments modified with PANI and from 398 μS cm^{-1} to 542 μS cm^{-1} for the pigments modified with PPY. The specific conductivities were higher at PVC = 5 % and lay within the ranges of 318 μS cm^{-1} to 443 μS cm^{-1} for PANI and from 503 μS cm^{-1} to 645 μS cm^{-1} for PPY. When the pigment concentrations were further increased to PVC = 10 % and to PVC = 15 %, the specific conductivities also increased, viz. to 348–1353 μS cm^{-1} and 465–1894 μS cm^{-1}, respectively, for PANI and to 461–887 μS.cm^{-1} and 521–1204 μS.cm^{-1}, respectively, for PPY. The higher specific conductivities of the aqueous extracts of the paint films with the pigments modified with the conductive polymers as compared to the untreated pigments was due to the presence of free charge carries on the polymeric chain, providing charge transfer across the chain. The positive charge at the chain is counterbalanced by the anion of the acid used for the protonation, i.e. phosphoric acid (and the phosphate anion derived from it) in this case. The layers of the conductive polymers undergo partial deprotonation in aqueous solutions (Kohl & Kalendová, 2014). The extent of release and deprotonation of increased amounts of the conductive polymers in the paint films in aqueous systems was higher for paints with higher pigment concentrations (PVC). The lowest as well as the highest conductivities were observed for paint films containing pigments modified with PANI.

Results of the accelerated corrosion tests

The aim of the accelerated corrosion tests was to evaluate the efficiency of the paints containing the composite pigments in substrate metal protection against corrosion near the artificial cut through the paint film and on the metal surface, as well as their resistance to blistering near the cut and on the paint film surface, and ultimately to calculate the overall anticorrosion efficiency of the paint films on exposure to the aggressive test environments.

Cyclic corrosion test in mist of a salt electrolyte

The results of the corrosion test in which the paint films were exposed to the mist of a salt electrolyte, viz. $(NH_4)_2SO_4$, are listed in Table 9. Protection against steel panel corrosion was from 0.1 % to 1 % in the best cases. A corroded surface fraction as low as 0.03 % was only

achieved with the $SrTiO_3$/PPY pigment at PVC = 1 % and 5 %. A corroded surface fraction of 0.1 % was obtained when using the paints with $CaTiO_3$/PPY at PVC = 1 %, $SrMnO_3$/PPY at PVC = 5 %, and $SrTiO_3$/PANI at PVC = 1 % and 5 %.

Corrosion in the cut was not markedly dependent on the PVC level, it was slightly lower at PVC > 5 %. The paint films containing the composite pigments suppressed corrosion in the cut better than the reference paint, where corrosion propagated to a distance of 4.0–4.5 mm. Metal surface corrosion beneath the paint films was more severe at higher PVC levels. The paints' anticorrosion efficiency was high at PVC = 1–5 %.

In conclusion, the findings from the test in which the steel panels coated with the paint films were exposed to an atmosphere with a salt electrolyte for 1440 hours can be summarised as follows:

- Paint films providing high protection against substrate metal surface corrosion (corroded area fraction ≤ 0.1 %) contained the following composite pigments at the following concentrations: $SrTiO_3$/PANI at PVC = 1 % and 5 %; $CaTiO_3$/PPY at PVC = 1 %); $SrTiO_3$/PPY at PVC = 1 % and 5 %; and $SrMnO_3$/PPY at PVC = 5 %
- The following pigments were efficient at a concentration as low as PVC = 1 %: $CaTiO_3$/PANI ($E_{electrol}$ = 66), $SrTiO_3$/PANI ($E_{electrol}$ = 67), $CaTiO_3$/PPY ($E_{electrol}$ = 79), $SrTiO_3$/PPY ($E_{electrol}$ = 79) and $SrMnO_3$/PPY ($E_{electrol}$ = 84); all of them are more efficient than the reference paint (i.e. $E_{electrol}$ > 59)
- PPY was superior to PANI also in this test, although not to such an extent as in the preceding tests
- Paints that attained a higher overall anticorrosion efficiency than the reference paint ($E_{electrol}$ = 59) contained the following composite pigments at the following concentrations: $CaTiO_3$/PANI at PVC = 1 % and 5 %; $SrTiO_3$/PANI at PVC = 1 %, 5 % and 10 %; $SrMnO_3$/PANI at PVC = 15 %; $CaTiO_3$/PPY at PVC = 1 %, 5 % and 10 %; $SrTiO_3$/PPY at PVC = 1 %, 5 %, 10 %; and $SrMnO_3$/PPY at PVC = 1 %, 5 %, 10 %
- Paints with the pigments present at PVC = 15 that were more efficient than the reference paint (zinc phosphate as the pigment at PVC = 15 %, $E_{electrol}$ = 59) contained the following composite pigments: $SrTiO_3$/PPY ($E_{electrol}$ = 59) and $SrMnO_3$/PANI ($E_{electrol}$ = 73)
- Paints that exhibited low corrosion in the cut (to distances ≤ 0.5 mm), contained the following pigments at the following concentrations: $SrTiO_3$/PANI at PVC = 10 %

(corrosion in the cut 0 mm) and $SrMnO_3$/PPY at PVC = 5 % and 10 %, (corrosion in the cut 0.5 mm)

The anticorrosion efficiency of the paints containing $CaTiO_3$/PANI and $CaTiO_3$/PPY is graphically documented in Fig. 21.

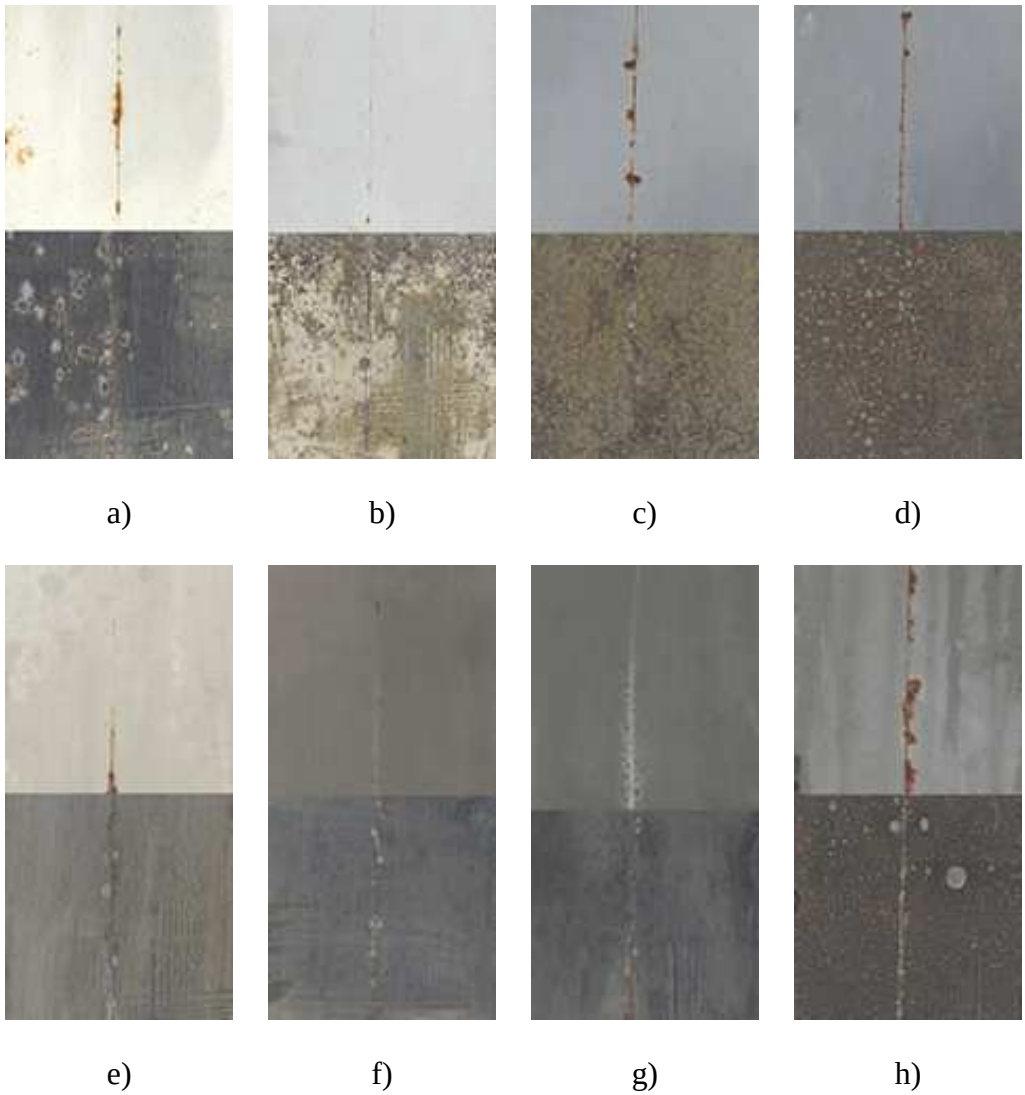

Fig. 21. Results of exposure of a steel panel coated with the paint containing $CaTiO_3$/PANI and $CaTiO_3$/PPY in mist of a salt electrolyte. Photographs of the bare and coated steel panels: status of the coating (top part of the panel) and of the substrate metal after removing the coating (bottom part of the panel). Paint with: a) pigment $CaTiO_3$/PANI at PVC= 1 %; b) pigment $CaTiO_3$/PANI at PVC = 5 %; c) pigment $CaTiO_3$/PANI at PVC = 10 %; d) pigment

$CaTiO_3$/PANI at PVC = 15 %; e) pigment $CaTiO_3$/PPY at PVC = 1%; f) pigment $CaTiO_3$/PPY at PVC = 5%; g) pigment $CaTiO_3$/PPY at PVC = 10%; h) pigment $CaTiO_3$/PPY at PVC = 15 %.

Linear polarisation

The parameters measured, i.e. the spontaneous corrosion potential, polarisation resistance and corrosion rate, provide information about the paint films' corrosion resistance (Table 10). A paint containing zinc phosphate at PVC = 15 % served as the reference material in the linear polarisation measurements.

The non-pigmented coating, with a spontaneous corrosion potential 42 mV, exhibited polarisation resistance of 3×10^6 Ω and corrosion rate 1×10^{-5} mm year^{-1}. The reference paint with zinc phosphate at PVC = 15 % exhibited a lower spontaneous corrosion potential, -473 mV, higher polarisation resistance, 3×10^7 Ω, and corrosion rate one order of magnitude lower, 1×10^{-6} mm year^{-1}. The two materials served as reference materials for the paint films containing the pigments modified the conductive polymers: $CaTiO_3$, $SrTiO_3$, $CaMnO_3$, $SrMnO_3$, Ca_2ZnWO_6 and Ca_2ZnMoO_6 at PVC = 1 %, 5 %, 10 % and 15 %.

The paint films with the $CaTiO_3$/PANI system exhibited spontaneous corrosion potential increase (-382 to -468 mV) against the reference paint with zinc phosphate. In comparison with the non-pigmented coating, the corrosion rate of this paint was lower only at PVC = 1 % and PVC = 5 %, viz. $v_{corr} = 8 \times 10^{-7}$ and 1×10^{-5} mm year^{-1}, respectively.

The paint films with the $CaTiO_3$/PPY system at PVC = 1 %, 5 % and 10 % exhibited spontaneous corrosion potentials higher than the reference paint film with zinc phosphate, viz. −175 to −354 mV. The spontaneous corrosion potential was lower, −600 mV, only at PVC = 15 %. The corrosion rate of the paint film at PVC = 1 % was nearly one-half that of the above reference paint, viz. 1×10^{-11} mm year^{-1}. The paint films containing this pigment at PVC = 5 and 10 % also exhibited appreciably lower corrosion rates, 5×10^{-9} and 2×10^{-8} mm year^{-1}, than the reference materials (non-pigmented coating and paint with zinc phosphate).

The paint films with $SrTiO_3$/PANI exhibited increase in the spontaneous corrosion potential against that of the reference zinc phosphate paint at PVC = 1 %, viz. −286 mV, whereas the reverse was true at PVC = 5 %, 10 % and 15 % (−635 mV to −587 mV). Also, the paint film with the pigment at PVC = 1 % was the only one in the increasing PVC series to exhibit a corrosion rate lower (8×10^{-7} mm year^{-1}) than the corrosion rate of the two reference materials.

The paint films with $SrTiO_3$/PPY exhibited spontaneous corrosion potential decrease (to −556 to −521 mV) compared to the reference paint film with zinc phosphate at any of the pigment concentrations used, and the corrosion rates at PVC = 1 % and 5 %, viz. 8×10^{-10} and 6×10^{-10} mm year^{-1}, respectively, were lower than the corrosion rate of the reference paint.

All of the paint films with the $CaMnO_3$/PANI and $SrMnO_3$/PANI systems exhibited spontaneous corrosion potential decrease against the reference paint with zinc phosphate; only the paint film with $CaMnO_3$/PANI at PVC = 1 % exhibited a corrosion rate at the same level as the reference paint film, viz. 1×10^{-6} mm year^{-1}.

All of the paint films with the $CaMnO_3$/PPY and $SrMnO_3$/PPY systems also exhibited spontaneous corrosion potential decrease against the reference paint with zinc phosphate (-576 to 483 mV), except for the paint films with $CaMnO_3$/PPY at PVC = 1 % and 5 %, where the spontaneous corrosion potential values were higher (−120 and −372 mV, respectively). The paint films with $CaMnO_3$/PPY at PVC = 1 % exhibited a lower corrosion rate than the reference paint with zinc phosphate, viz. 7×10^{-10} mm year^{-1}, and the same was true of the paints with $SrMnO_3$/PPY at PVC = 1 % and 5 % (7×10^{-7} and 2×10^{-8} mm year^{-1}, respectively).

Physico-mechanical tests of the paint films

Tests were also performed to examine the paints' adhesion-barrier properties. The factors measured included adhesion to the substrate, hardness, and strength. Because unsupported paint films are difficult to prepare, the properties of the paints were measured directly on metal substrates in accordance with standardised tests. The tests imitate mechanical stresses in the external environment, such as an object being dropped onto the surface (impact test) and deformations caused by bending and elongation (bending test and cupping test). The aim was to determine the degree of paint adhesion, paint resistance to cupping, resistance to dropping weight impact from the reverse side and from the averse side, and resistance to bending over a cylindrical mandrel. The overall mechanical resistance was high for all of the paint films studied (Table 11). The paint films with higher PVC levels were more plastic, their overall physico-mechanical resistance was nearly 100 %. The mechanical resistance of the paints containing the composite pigments at PVC = 15 % was higher than that of the reference paint with zinc phosphate at the same pigment concentration. All of the paint films remained undamaged in the test in which a 1000 g weight was dropped onto the averse side of the painted panel from a height of 100 cm, and their resistance was better at higher PVC levels. The best results (100 % resistance) were obtained with the paints containing the composite pigment

$SrTiO_3$/PPY, particularly at PVC = 10 % and 15 %. Nearly all of the paints were highly resistant to bending over a mandrel 4 mm in diameter. Adhesion of all the paints exhibited a value of 0. From the evaluation of the physico-mechanical tests it follows that the film possessing the higher of the PVC levels applied often possessed a nearly 100 % physico-mechanical resistance. This (i.e. 100 % resistance) was true, in particular, of the paints containing the following composite pigments: $CaTiO_3$/PANI at PVC = 10 %; $SrTiO_3$/PANI at PVC = 10 %; $SrTiO_3$/PPY at PVC = 10 % and 15 %; $CaMnO_3$/PANI at PVC = 15 %; and $SrMnO_3$/PANI at PVC = 15 %. The paints containing the pigments at PVC = 15 % exhibited overall mechanical resistance values comparable to or higher than that of the reference paint.

Anticorrosion effect of perovskites and conductive polymers in a paint layer

In recent years, application of conductive polymer coatings such as polypyrrole (PPY) and polyaniline (PANI) on ferrous and non-ferrous alloys against corrosion has received much attention (Li et al., 2005; Özyılmaz, et al., 2004). In addition to applying the physical barrier, which is the protection mechanism of most coatings, the conductive polymers are capable to anodic protection of metal surface by the healing their oxidative properties and accelerating the formation of stable metal oxides on the surface of the substrate (Nguyen et al., 2004; Tallman et al., 2002). In other words, the ability of the conducting polymer to oxidize the substrate metals allows potential of metals to be shifted to the passive state, in which the metals are protected by the passive oxide formed beneath the conducting polymer. The application of the conducting polymer coating to the corrosion protection of steels was reviewed by Tallman et al. (2002).

The mechanism of action of the conductive PANI species at the metal/organic coating interface is shown in Fig. 2. Iron is directly oxidised to Fe 3+ ions. (Passivating layers with Fe(III) are less soluble and hence more resistant than passivating layers with Fe(II).) This direct oxidation is accelerated by the catalytic redox effect of PANI (ES = protonated emeraldine, LE = leucoemeraldine, and EB = emeraldine base). The oxidising power of PANI is affected appreciably by the dopant type (Rout et al., 2003; Wessling, 1997). The effect of PPY in the paint layer is explained likewise.

Where the pigment particle is not modified with a conductive polymer layer, the anticorrosion protection role is played by the inorganic pigment itself.

Conclusions

PPY as the conductive polymer for pigment particle surface modification was found superior to PANI with respect to the corrosion-inhibiting efficiency of the composite pigments. It is an advantage that a low pigment volume concentration in the epoxy-ester resin based paint is adequate to attain a high anticorrosion efficiency. The pigments with PPY exhibited more favourable physico-chemical properties (water-soluble content, pH of the extracts), which did not detract from the binder's barrier efficiency. For some of the pigments, their optimum concentration in the paints was as low as PVC = 1 %, which is beneficial also from the financial aspect.

When exposed to the atmosphere with the salt electrolyte, the paint films exhibited an anticorrosion effect particularly at low PVC levels (1% and 5%).

All of the paint films exhibited a high anticorrosion resistance in this chamber; excellent results were obtained with the paints containing PPY. Specifically, they were paints containing $SrMnO_3$/PPY at PVC = 1% and 5%, where the overall anticorrosion efficiency score was 92%.

PPY appeared to be superior to PANI also in the linear polarisation measurements, and lower concentrations of the pigments coated with PPY were more efficient than high concentrations. Paint films with the following composite pigments exhibited better resistance and lower corrosion rates than the reference paint with the zinc phosphate pigment. Efficient paints, based on the linear polarisation measurements and the accelerated corrosion test of the paints containing composite pigments in mist of a salt electrolyte, were those containing the $CaTiO_3$/PPY composite pigment and the $SrTiO_3$/PPY composite pigment.

All of the paints with the pigments modified with the conductive polymers exhibited good physico-mechanical resistance levels - to the extent that the paints are applicable to surfaces exposed to mechanical stresses.

The surface modified pigments are promising from several aspects, particularly owing to their high anticorrosion efficiency compared to that of the reference paint, low pigment concentration in the paints adequate to attain a high anticorrosion effect, and their environmental harmlessness. The results obtained suggest that the pigments deserve further research.

Symbols

ABO_3	the general structure perovskite
ASTM	American Standard for Testing and Materials

B	the Stern-Geary coefficient	mV
CP	conductive polymers	
$CPVC$	critical pigment volume concentration	%
CSN	czech state norm	
D	dense (the highest frequency of the blistering of paint)	
DFT	dry film thickness	
e^-	electron	
e.g.	exempli gratia	
EB	emeraldine base	
E_{corr}	spontaneous corrosion potential	mV
$E_{electrol}$	overall anticorrosion efficiency	
E_{OC}	potential value reached at the end of the previous open circuit period	mV
ES	emeraldine salt	
F	Faraday constant (96485)	C mol^{-1}
F	few (the lowest frequency of the blistering of paint)	
Fe	iron	
H	hydrogen	
HA	hydrogen acid	
i.e.	id est	
I_{corr}	current density	mV
ISE	ion-selective electrode	
ISO	International Organization for Standardization	
LE	leucoemeraldine	
M	molecular weight of the panel material (= 55.85 g $mol^{-1}$for Fe)	g mol^{-1}
M	medium (frequency of the blistering of paint)	
MD	medium dense (frequency of the blistering of paint)	
oil abs	oil absorption	g $100g^{-1}$
PANI	polyaniline phosphate	
PPY	polypyrrole phosphate	
PVC	pigment volume concentration	%
R_p	polarisation resistance	Ω
SCE	saturated calomel electrode	
SEI	secondary electron imaging	
SEM	Scanning Electron Microscope	

t	time	s
W_{20}	water-soluble fraction	%
XRD	X-ray diffraction	
XRF	X-ray fluorescence	
XYO_3	the perovskite type pigments (X = Zn, Ca Sr, Y = Ti, Mn)	
z	number of electrons involved in the $Fe^0 \rightarrow Fe^{2+} + 2\ e^-$ reaction	

Greek Letters

β_a	tafel region slopem	mV
β_c	tafel region slopem	mV
ρ	density	g cm^{-3}
ρ_{Fe}	density	g cm^{-3}
υ_{corr}	corrosion rate	mm $year^{-1}$
χ	conductivity	mS cm^{-1}

Subscripts

a	anode
c	cathode
corr	corrosion
electrol	mist of a salt electrolyte
Fe	iron
oc	open circuit period
p	polarization
electrol	mist of a salt electrolyte
f	film
p	pigment

References

Ahmad, N., & MacDiarmid, A. G. (1996). Inhibition of corrosion of steels with the exploitation of conducting polymers. *Synthetic Metals, 78,* 103–110. DOI: 10.1016/0379-6779(96)80109-3.

Ahmed, N. M., Mohamed, M. G., Mabrouk M. R., & ELShami, A. A. (2015). Novel anticorrosive pigments based on waste material for corrosion protection of reinforced concrete steel. *Construction and Building Materials, 98,* 388–396. DOI: 10.1016/j.conbuildmat.2015.08.111.

Alizahed, R., Beaudoin, J. J., Ramachandran, V.S., & Raki, L. (2009). Applicability of the Hedvall effect to study the reactivity of calcium silicate hydrates. *Advances in Cement Research, 21,* 59–66. DOI: 10.1680/adcr.2008.00008.

Armelin, E., Alemán, C., & Iribarren, J. I. (2009). Anticorrosion performances of epoxy coatings modified with polyaniline: A comparison between the emeraldine base and salt forms. *Progress in Organic Coatings, 65,* 88–93. DOI: 10.1016/j.porgcoat.2008.10.001.

Armelin, E., Pla, R., Liesa, F., Ramis. X., Iribarren J. I., & Alemán, C. (2008). Corrosion protection with polyaniline and polypyrrole as anticorrosive additives for epoxy paint. *Corrosion Science, 50,* 721–728. DOI: 10.1016/j.corsci.2007.10.006.

Brodinová, J., Stejskal, J., & Kalendová, A. (2007). Investigation of ferrites properties with polyaniline layer in anticorrosive coatings. *Journal of Physics and Chemistry of Solids, 68,* 1091–1095. DOI: 10.1016/j.jpcs.2006.11.018.

Choudhary, V. R., Banerjee, S., & Uphade, B. S. (2000). Activation by hydrothermal treatment of low surface area ABO_3-type perovskite oxide catalysts. *Applied Catalysis A: General, 197,* 183–186. DOI: 10.1016/S0926-860X(99)00485-8.

Criado, M., Sobrados, I., Bastidas, J. M., & Sanz, J. (2015). Steel corrosion in simulated carbonated concrete pore solution its protection using sol-gel coatings. *Progress in Organic Coatings, 88,* 228–236. DOI: 10.1016/j.porgcoat.2015.06.002.

Deya, M. C., Blustein, G., Romagnoli, R., Sarli, A. R. D., & Amo, B. (2002). The influence of the anion type on the anticorrosive behaviour of inorganic phosphates. *Surface and Coatings Technology, 150,* 133–142. DOI: 10.1016/S0257-8972(01)01522-5.

Fang, J., Xu, K., & Zhu, L. X. (2007). A study on mechanism of corrosion protection of polyaniline coating and its failure. *Corrosion Science, 49,* 4232–4242. DOI: 10.1016/j.corsci.2007.05.017.

Feng, L. M., Jiang, L. Q., Zhu, M., Liu, H. B., Zhou, X., & Li, C. H. (2008). Formability of ABO_3 cubic perovskites. *Journal of Physics and Chemistry of Solids, 69,* 967–974. DOI: 10.1016/j.jpcs.2007.11.007.

Goldschmidt, A., & Streitberger, H. J. (2007). *BASF Handbook on Basics of Coating Technology (*pp. 345–401). Vincentz Network: Germany. ISBN 973-3-86630-903-6.

Granizo, N., Vega, J. M., Fuente, D., Chico, B., & Morcillo, M. (2013). Ion-exchange pigments in primer paints for anticorrosive protection of steel in atmospheric service: Anion-exchange pigments. *Progress in Organic Coatings, 76,* 411–424. DOI: 10.1016/j.porgcoat.2012.10.009.

Grgur, B. N., Elkais, A. R., Gvozdenović, M. M. S., Drmanić, Ž., Trišović, T. Lj., & Jugović, B. Z. (2015). Corrosion of mild steel with composite polyaniline coatings using different formulations. *Progress in Organic Coatings, 79,* 17–24. DOI: 10.1016/j.porgcoat.2014.10.013.

Kalendová, A. (2000). Alkalising and neutralising effects of anticorrosive pigments containing Zn, Mg, Ca, and Sr cations. *Progress in Organic Coatings, 38,* 199–206. DOI: 10.1016/S0300-9440(00)00103-X.

Kalendová, A. (2003). Effects of particle sizes and shapes of zinc metal on the properties of anticorrosive coatings. *Progress in Organic Coatings, 46,* 324–332. DOI: 10.1016/S0300-9440(03)00022-5.

Kalendová, A., Veselý, D., & Stejskal, J. (2008a). Organic coatings containing polyaniline and inorganic pigments as corrosion inhibitors. *Progress in Organic Coatings, 62,* 105–116. DOI: 10.1016/j.porgcoat.2007.10.001.

Kalendová, A., Sapurina, I., Stejskal, J., & Veselý, D. (2008b). Anticorrosion properties of polyaniline-coated pigments in organic coatings. *Corrosion Science, 50,* 3549–3560. DOI: 10.1016/j.corsci.2008.08.044.

Kalendová, A., & Veselý, D. (2009). Study of the anticorrosive efficiency of zincite and periclase-based core-shell pigments in organic coatings. *Progress in Organic Coatings, 64,* 5–19. DOI: 10.1016/j.porgcoat.2008.07.003.

Kalendová, A., Veselý, D., & Kalenda, P. (2010). Properties of paints with hematite coated muscovite and talc particles. *Applied Clay Science, 48,* 581–588. DOI: 10.1016/j.clay.2010.03.007.

Kalendová, A., Veselý, D., Kohl, M., & Stejskal, J. (2014a). Effect of surface treatment of pigment particles with polypyrrole and polyaniline phosphate on their corrosion inhibiting properties in organic coatings. *Progress in Organic Coatings, 77,* 1465–1483. DOI: 10.1016/j.porgcoat.2014.04.012.

Kalendová, A., Veselý, D., & Kohl, M. (2014b). Synthesis of Me_2TiO_4 and $MeFe_2O_4$ spinels and their use in organic alkyd resin-based anticorrosion coatings. *Corrosion Review*, *32*, 51–72. DOI 10.1515/corrrev-2013-0050.

Kalendová, A., Hejdová, M., & Veselý, D. (2015a). Investigation of the anticorossion properties of perovskites in epoxy-ester resin based organic coating materials. *Anti-Corrosion Methods and Materials, 62,* 197–211. DOI: 10.1108/ACMM-01-2014-1344.

Kalendová, A. Veselý, D. Kohl, M. & Stejskal, J. (2015b). Anticorrosion efficiency of zinc-filled epoxy coatings containing conducting polymers and pigments. *Progress in Organic Coatings, 78,* 1–20. DOI: 10.1016/j.porgcoat.2014.10.009.

Király, A., & Ronkay, F. (2015). Temperature dependence of electrical properties in conductive polymer composites. *Polymer Testing, 43,* 154–162. DOI: 10.1016/j.polymertesting.2015.03.011.

Kohl, M., & Kalendová, A. (2014). Assessment of the impact of polyaniline salts on corrosion properties of organic coatings. *Koroze a ochrana materiálu, 58*, 113–119. DOI: 10.1515/kom-2015-0004.

Kouřil, M., Novák, P., & Bojko, M. (2006). Limitations of the linear polarization method to determine stainless steel corrosion rate in concrete environment. *Cement & Concrete Composites, 28,* 220–225. DOI: 10.1016/j.cemconcomp.2006.01.007.

Kreutz, E. W., & Gottmann, J. (2004). PLD of perovskite coatings for optoelectronics, microelectronics, and microtechnology. *Journal of the European Ceramic Society, 24,* 979–984. DOI: 10.1016/S0955-2219(03)00514-4.

Li, C. M., Sun, C. Q., Chen, W., & Pan, L. (2005). Electrochemical thin film deposition of polypyrrole on different substrates. *Surface & Coatings Technology, 198,* 474–477. DOI: 10.1016/j.surfcoat.2004.10.065.

Lu, W. K., Elsenbaumer, R. L., & Wessling, B. (1995). Corrosion protection of mild steel by coatings containing polyaniline. *Synthetic Metals, 71,* 2163–2166. DOI: 10.1016/0379-6779(94)03204-J.

Millard, S. G., Law, D., Bungey, J. H., & Cairns, J. (2001). Environmental influences on linear polarisation corrosion rate measurement in reinforced concrete. *NDT&E International, 34,* 409–417. DOI: 10.1016/S0963-8695(01)00008-1.

Mostafaei, A., & Nasirpouri, F. (2014). Epoxy/polyaniline-ZnO nanorods hybrid nanocomposite coatings: Synthesis, characterization and corrosion protection performance of conducting paints. *Progress in Organic Coatings, 77,* 146–159. DOI: 10.1016/j.porgcoat.2013.08.015.

Naderi, R., Arman, S. Y., & Fouladvand, Sh. (2014). Investigation on the inhibition synergism of new generations of phosphate-based anticorrosion pigments. *Dyes and Pigments, 105,* 23–33. DOI: 10.1016/j.dyepig.2014.01.015.

Navarchian, A. H., Joulazadeh, M., & Karimi., F. (2014). Investigation of corrosion protection performance of epoxy coatings modified by polyaniline/clay nanocomposites on steel surfaces. *Progress in Organic Coatings, 77,* 347–353. DOI:10.1016/j.porgcoat.2013.10.008.

Nguyen, T. D., Nguyen, T. A., Pham, M. C., Piro, B., Normand, B., & Takenouti, H. (2004). Mechanism for protection of iron corrosion by an intrinsically electronic conducting polymer. *Journal of Electroanalytical Chemistry, 572,* 225–234. DOI: 10.1016/j.jelechem.2003.09.028.

Özyilmaz, A. T., Tüken, T., Yazici, B., & Erbil, M. (2004). The electrochemical synthesis and corrosion performance of polypyrrole on brass and copper. *Progress in Organic Coatings, 51,* 152–160. DOI: 10.1016/j.porgcoat.2004.09.003.

Patil, R. S., & Radhakrishnan, S. (2006). Conducting polymer based hybrid nano-composites for enhanced corrosion protective coatings. *Progress in Organic Coatings, 57,* 332–336. DOI:10.1016/j.porgcoat.2006.09.012.

Rout, T. K., Jha, G., Singh, A. K., Bandyopadhyay, N., & Mohantzy, O. N. (2003). Development of conducting polyaniline coating: a novel approach to superior corrosion resistence. *Surface and Coatings Technology, 167,* 16–24. DOI: 10.1016/S0257-8972(02)00862-9.

Sangaj, S. S., & Malshe, V. C. (2004). Permeability of polymers in protective organic coatings. *Progress in Organic Coatings,* 28–39. DOI: 10.1016/j.porgcoat.2003.09.015.

Somboonsub, B., Srisuwan, S., Invernale, M. A., Thongyai, S., Praserthdam, P., Scola, D. A., & Sotzing, G. A. (2010). Comparison of the thermally stable conducting polymers PEDOT, PANi, and PPy using sulfonated poly(imide) templates. *Polymer, 51,* 4472–4476. DOI: 10.1016/j.polymer.2010.08.008.

Tallman, D., Spinks, G., Dominis, A., & Wallace G. (2002). Electroactive conducting polymers for corrosion control. *Journal of Solid State Electrochemistry, 6,* 73–84. DOI:10.1007/s100080100212.

Trojan, M., Brandova, D., & Solc, Z. (1987). Study of the thermal preparation and stability of tetrametaphosphates of bivalent metals. *Thermochimica Acta, 110,* 343–358. DOI: 10.1016/0040-6031(87)88244-8.

Vakili, H., Ramezanzadeh, B., & Amini, R. (2015). The corrosion performance and adhesion properties of the epoxy coating applied on the steel substrates treated by cerium-based conversion coatings. *Corrosion Science, 94,* 466–475. DOI: 10.1016/j.corsci.2015.02.028.

Veselý, D., Kalendová, A., & Kalenda, P. (2010). A study of diatomite and calcined kaoline properties in anticorrosion protective coatings. *Progress in Organic Coatings, 68,* 173–179. DOI: 10.1016/j.porgcoat.2010.02.007.

Veselý, D., Kalendová, A., & Manso, M. V. (2012). Properties of calcined kaolins in anticorrosion paints depending on PVC, chemical composition and shape of particles, *Progress in Organic Coatings, 74,* 82–91. DOI: 10.1016/j.porgcoat.2011.11.017.

Vliet, C. H. (1998). Reduction of zinc and volatile organic solvents in two-pack anti- corrosive primers, a pilot study. *Progress in Organic Coatings, 34*, 220–226. DOI: 10.1016/S0300-9440(98)00027-7.

Wessling, B., Schröder, S., Gleeson, S., Merkle, H., Schröder, S., & Baron, F. (1996) Reaction scheme for the passivation of metals by polyaniline. *Materials and Corrosion, 47,* 439–445.

Wessling, B. (1997). Scientific and Commercial Breakthrough for Organic Metals. *Synthetic Metals, 85,* 1313–1318. DOI: 10.1016/S0379-6779(97)80254-8.

Wessling, B., & Posdorfer, J. (1999). Nanostructures of the dispersed organic metal polyaniline responsible for macroscopic effects in corrosion protection. *Synthetic Metals, 102,* 1400–1401. DOI 10.1016/S0379-6779(98)01059-5.

Yang, W., Li, Q., Xiao, Q., & Liang, J. (2015). Improvement of corrosion protective performance of organic coating on low carbon steel by PEO pretreatment. *Progress in Organic Coatings, 89,* 260–266. DOI: 10.1016/j.porgcoat.2015.09.003.

Zubielewicz, M., & Gnot, W. (2004). Mechanisms of non-toxic anticorrosive pigments in organic waterborne coatings. *Progress in Organic Coatings, 49,* 358–371. DOI: 10.1016/j.porgcoat.2003.11.001.